AD-A177 360

20030128106

AD_____

USE OF NUCLEIC ACID-PROTEIN CYTOPHOTOMETRY AND CYTOINTERFEROMETRY IN CHARACTERIZING CELLULAR MODE OF TRICHOTHECENE TOXICANT ACTION

Final Report

Adam Anthony, Theodore M. Hollis

and Lee Martin

October 1986

DTIC
ELECTE
FEB 2 6 1987
S D
D

Supported by

U. S. ARMY MEDICAL RESEARCH DEVELOPMENT COMMAND

Fort Detrick, Frederick, Maryland 21701-5012

Contract No. DAMD17-86-C-6101
The Pennsylvania State University
University Park, Pennsylvania 16802

Approved for public release; distribution unlimited

DTIC FILE COPY

The views, opinions, and/or findings contained in this report are not to be construed as an official Department of Army position, policy or decision unless so designated by other documentation.

87 2 25 14

SECURITY CLASSIFICATION OF THIS PAGE (When Data Entered)

REPORT DOCUMENTATION PAGE	READ INSTRUCTIONS BEFORE COMPLETING FORM
1. REPORT NUMBER	2. GOVT ACCESSION NO. ADA177360 — 3. RECIPIENT'S CATALOG NUMBER
4. TITLE (and Subtitle): Use of Nucleic Acid-Protein Cytophotometry and Cytointerferometry in Characterizing Cellular Mode of Trichothecene Toxicant Action	5. TYPE OF REPORT & PERIOD COVERED: FINAL REPORT 1 Feb. 1986 - 30 Sept. 1986 — 6. PERFORMING ORG. REPORT NUMBER
7. AUTHOR(s): Adam Anthony, Theodore M. Hollis and Lee J. Martin	8. CONTRACT OR GRANT NUMBER(s): DAMD17-86-C-6101
9. PERFORMING ORGANIZATION NAME AND ADDRESS: The Pennsylvania State University, College of Science, Biology Department, University Park, PA 16802	10. PROGRAM ELEMENT, PROJECT, TASK AREA & WORK UNIT NUMBERS: 61102A.3M161102BS12.AA.129
11. CONTROLLING OFFICE NAME AND ADDRESS: U.S. Army Medical Research & Development Command, Fort Detrick, Frederick, MD 21701-5012	12. REPORT DATE: October, 1986 — 13. NUMBER OF PAGES: 71 — 14. SECURITY CLASS. (of this report): Unclassified — 15a. DECLASSIFICATION/DOWNGRADING SCHEDULE

16. DISTRIBUTION STATEMENT (of this Report)

Approved for public release; distribution unlimited

17. DISTRIBUTION STATEMENT (of the abstract entered in Block 20, if different from Report)

18. SUPPLEMENTARY NOTES

19. KEY WORDS (Continue on reverse side if necessary and identify by block number)

Toxicity, T-2 toxin, cardiotoxicity, myocardial RNA-protein, enterotoxicity, hepatotoxicity, neuropathology, nucleic acid histochemistry, corticosterone, histamine, endothelial cell injury, mast cells, azure B-RNA, Feulgen-DNA, Coomassie blue-protein, cytophotometry, scanning-integrating microdensitometry

20. ABSTRACT (Continue on reverse side if necessary and identify by block number)

Cytophotometric analyses were made of nucleic acid-protein responses in known and putative target tissues of adult male Sprague-Dawley rats injected intraperitoneally with T-2 toxin, a small molecular weight trichothecene mycotoxin at dosages of 0.75, 1.0, 1.5 and 6.0 mg/kg (1 LD_{50} = 0.9 mg/kg). Animals were decapitated during acute (2-8 h) or delayed (7-28 d) intervals after exposure. Tissues removed and processed for subsequent microchemical and cytomorphological analyses included the heart, cecum, liver, kidney,

DD FORM 1 JAN 73 1473 EDITION OF 1 NOV 65 IS OBSOLETE

Unclassified

SECURITY CLASSIFICATION OF THIS PAGE (When Data Entered)

lungs, spleen, thymus, adrenals and mesenteric spreads. Cellular RNA and protein levels were assayed using azure B-RNA and Coomassie-protein cytophotometry; DNA and chromatin alterations were quantified using Feulgen-DNA cytophotometry and ocular filar micrometry. Correlative biochemical data were obtained on changes in circulating histamine and corticosterone levels. In vitro studies were also conducted of nucleic acid-protein responses of cultured endothelial cells subjected to T-2 toxin using pyronin Y-fluorescence, flow cytofluorometry, azure B-RNA cytophotometry and cytointerferometric assay of protein. Major findings supported by the overall study are as follows:

(1) Both in vivo and in vitro studies indicate the arteriovascular endothelial cell is highly susceptible to T-2 toxin-induced cytotoxicity. Endothelial cell injury thus constitutes the initial event which precipitates subsequent pathogenic effects in major target sites of T-2 toxin action.

(2) The heart and intestine constitute major target sites of acute T-2 toxin poisoning. Specific cardiotoxic manifestations include endothelial disruption, edema and depletion of myocardial protein content. Major enterotoxic effects include edema and lesion formation in germinal centers of Peyers patches and disruption of crypt epithelium.

(3) Although the kidney and liver of T-2 toxin challenged rats exhibit moderate extents of cellular injury, these appear to be less prone to injury than cardiovascular, enteric or hemopoietic tissue compartments.

(4) Massive degranulation of mast cells and elevated plasma histamine levels are an important aspect of T-2 toxin poisoning and probably exacerbate the extent of toxin-induced impairment in cardiovascular functioning. The absence of a toxin-induced elevation in corticosterone release may also be a contributing factor in making vascular endothelial cell membranes more prone to injury.

(5) With respect to immunotoxic effects of T-2 toxin, it appears that B-dependent lymphoidal compartments are more severely affected than T-dependent regions. This suggests that a suppression of humoral (antigen-antibody) defense mechanisms is more severe than impairment of cell mediated lymphocytic immune responses.

(6) In most major and secondary target sites, inhibition of protein synthesis is the primary cellular mechanism of T-2 toxicant action, since the extent of protein depletion is more severe and often precedes suppression of RNA synthesis and/or the inhibition of chromatin template activity. However, in some cells such as the mast cells and arterial endothelial cells, cytotoxic effects of T-2 toxin probably stem from direct injury to the plasma membrane.

AD_____

USE OF NUCLEIC ACID-PROTEIN CYTOPHOTOMETRY AND CYTOINTERFEROMETRY IN CHARACTERIZING CELLULAR MODE OF TRICHOTHECENE TOXICANT ACTION

Final Report

Adam Anthony, Theodore M. Hollis

and Lee Martin

October 1986

Supported by

U. S. ARMY MEDICAL RESEARCH DEVELOPMENT COMMAND

Fort Detrick, Frederick, Maryland 21701 -5012

Contract No. DAMD17-86-C-6101
The Pennsylvania State University
University Park, Pennsylvania 16802

Approved for public release; distribution unlimited

The views, opinions, and/or findings contained in this report are not to be construed as an official Department of Army position, policy or decision unless so designated by other documentation.

Accesion For
NTIS CRA&I ☑
DTIC TAB ☐
Unannounced ☐
Justification .....
By .....
Distribution /
Availability Codes
Dist | Avail and / or Special
A-1

DTIC COPY INSPECTED

List of Publications supported in part by Contract No. DAMD17-86-C-6101

Martin, L.J., J.A. Doebler and A. Anthony. 1986. Scanning cytophotometric analysis of brain neuronal nuclear chromatin changes in acute T-2 toxin-treated rats. Toxicol. Appl. Pharmacol. 85:207-214.

Martin, L.J., J.D. Morse and A. Anthony. 1986. Quantitative cytophotometric analysis of brain neuronal RNA and protein changes in acute T-2 mycotoxin poisoned rats. Toxicon (in press).

List of personnel receiving contract support

Adam Anthony, Ph.D., Principal Investigator
Theodore M. Hollis, Ph.D., Coinvestigator
Lee J. Martin, Ph.D., Research Assistant
Young Kim, M.S.
Gary Pritchard, M.S.
Laura Golden, B.S.
Joseph Morse, B.S.

SUMMARY

Cytophotometric analyses were made of nucleic acid-protein responses in known and putative target tissues of adult male Sprague-Dawley rats injected intraperitoneally with T-2 toxin, a small molecular weight trichothecene mycotoxin at dosages of 0.75, 1.0, 1.5 and 6.0 mg/kg (1 LD_{50} = 0.9 mg/kg). Animals were decapitated during acute (2-8 h) or delayed (7-28 d) intervals after exposure. Tissues removed and processed for subsequent microchemical and cytomorphological analyses included the heart, cecum, liver, kidney, lungs, spleen, thymus, adrenals and mesenteric spreads. Cellular RNA and protein levels were assayed using azure B-RNA and Coomassie-protein cytophotometry; DNA and chromatin alterations were quantified using Feulgen-DNA cytophotometry and ocular filar micrometry. Correlative biochemical data were obtained on changes in circulating histamine and corticosterone levels. In vitro studies were also conducted of nucleic acid-protein responses of cultured endothelial cells subjected to T-2 toxin using pyronin Y-fluorescence, flow cytofluorometry, azure B-RNA cytophotometry and cytointerferometric assay of protein. Major findings supported by the overall study are as follows:

(1) Both in vivo and in vitro studies indicate the arteriovascular endothelial cell is highly susceptible to T-2 toxin induced cytotoxicity. Endothelial cell injury thus constitutes the initial event which precipitates subsequent pathogenic effects in major target sites of T-2 toxin action.

(2) The heart and intestine constitute major target sites of acute T-2 toxin poisoning. Specific cardiotoxic manifestations include endothelial disruption, edema and depletion of myocardial protein content. Major enterotoxic effects include edema and lesion formation in germinal centers of Peyers patches and disruption of crypt epithelium.

(3) Although the kidney and liver of T-2 toxin challenged rats exhibit moderate extents of cellular injury, these appear to be less prone to injury than cardiovascular, enteric or hemopoietic tissue compartments.

(4) Massive degranulation of mast cells and elevated plasma histamine levels are an important aspect of T-2 toxin poisoning and probably exacerbate the extent of toxin-induced impairment in cardiovascular functioning. The absence of a toxin-induced elevation in corticosterone release may also be a contributing factor in making vascular endothelial cell membranes more prone to injury.

(5) With respect to immunotoxic effects of T-2 toxin, it appears that B-dependent lymphoidal compartments are more severely affected than T-dependent regions. This suggests that a suppression of humoral (antigen-antibody) defense mechanisms is more severe than impairment of cell mediated lymphocytic immune responses.

(6) In most major and secondary target sites, inhibition of protein synthesis is the primary cellular mechanism of T-2 toxicant action, since the extent of protein depletion is more severe and often precedes suppression of RNA synthesis and/or the inhibition of chromatin template activity. However, in some cells such as the mast cells and arterial endothelial cells, cytotoxic effects of T-2 toxin probably stem from direct injury to the plasma membrane.

FOREWORD

The research described herein was conducted during the 1 February 1986 to 30 September 1986 interval and was supported by the U.S. Army Medical Research and Development Command under contract No. DAMD 17-86-C-6101, project title: "Use of Nucleic Acid - Protein Cytophotometry and Cytointerferometry in Characterizing Cellular Mode of Trichothecene Toxicant Action". The Principal Investigator of this contract was Adam Anthony, Ph.D., Professor of Zoology, with Dr. T. M. Hollis acting as coinvestigator and Lee J. Martin, Ph.D., as Research Associate and Project Assistant.

Acronyms and other scientific terms (indicated by the symbol † when first used) are defined in the glossary. Consecutive numbers are used for text citations. Publications, list of personnel receiving contract support and individuals receiving graduate degrees whose work was supported in part by the subject contract are included on page 5.

All microscopic and analytical histochemical analyses of tissues from T-2 toxin treated rats were carried out in the Histochemistry-Physiology Laboratories, Department of Biology, The Pennsylvania State University, University Park, PA 16802.

Personnel who actively participated in various aspects of this research include Adam Anthony, Ph.D., Theodore M. Hollis, Ph.D., Lee J. Martin, Ph.D., Jeffrey Doebler, Ph.D., Young Kim, M.S., Gary Pritchard, M.S., Kraig Sturtz, M.S., Tracy Collins, M.S., Patricia Wilson Witherspoon, M.S., Joseph Iobst, M.S., Robert Fanning, M.S., Earl Nollenberger, D.Ed., Joseph Morse, B.S., David Cherniak, B.S., and Mark Hoover, B.S. We also wish to acknowledge Randal Blank, Ph.D., who aided in the histamine analyses and in vitro cytofluorometric assay of nucleic acid responses in T-2 treated cell cultures. Special recognition is given to Mrs. Mary Alice Shea for typing and editorial assistance.

Citations of trade names and commercial organizations in this report do not constitute an official Department of the Army endorsement of the products or services of these organizations.

In conducting the research described in this report, the investigators adhered to the "Guide for the Care and Use of Laboratory Animals" of the National Institutes of Health, NIH Publication No. 85-23 (Revised 1985).

TABLE OF CONTENTS

LIST OF TABLES

LIST OF TABLES (Continued)

LIST OF FIGURES

BODY OF REPORT

(1) Statement of the Problem

It is well documented that trichothecenes, including T-2 toxin†, elicit a diverse array of pathological responses in cardiovascular, hemopoietic, gastrointestinal, neural, endocrine and reproductive tissue compartments. The most severe cytotoxic alterations occur in tissues with actively dividing cells and reportedly stem from an inhibition of protein synthesis. However, large gaps exist in our understanding of primary versus secondary target sites of intoxication and the time-course of pathogenesis in such compartments. Especially lacking are *in vivo* studies of T-2 toxin-induced cardiotoxic alterations in relation to impairments in functioning of other homeostatic organ systems within the same animal.

Thus, a major focus of the present study was on characterizing T-2 toxin induced alterations in regulatory aspects of macromolecular biosynthesis in cardiovascular cell elements using *in vivo* and *in vitro* model systems. Correlative *in vivo* studies were also undertaken of nucleic acid-protein changes in neural, adrenocortical, hepatic, intestinal and other tissue compartments to obtain a more comprehensive assessment of the overall systemic organ-system responses associated with acute and delayed T-2 toxin poisoning.

The scope of work and specific objectives involved the following:

1. Quantification of chromatin, RNA† and protein changes in myocardial cell elements following both *in vivo* and *in vitro* T-2 toxin exposure. The aim of this phase of work was to determine whether the heart constitutes a primary target site of T-2 toxin action; also to identify specific cell types prone to injury and obtain insight relating to the cellular mode of action.

2. Characterization of dose-dependent cytopathic and nucleic acid-protein changes in brain, liver, kidney, intestinal and adrenal tissue compartments. The aim of this phase of the study was to ascertain the minimum effective dosages of T-2 toxin which elicit acute or subacute cytomorphologic or biochemical (e.g. RNA-protein depletion) lesions in putative target sites of toxicant action.

3. Supplemental data were also collected on overt behavioral responses, circulating corticosterone and histamine levels, mesenteric mast cell degranulation and physiological parameters such as blood pressure to further elucidate the systemic and cellular mechanisms which precipitate cardiovascular shock.

---

†Terms followed by daggers are defined in the Glossary, p 67

The major analytical approach entailed use of scanning-integrating microchemical cytophotometric assay of chromatin, DNA†, RNA and protein changes in microscopically defined regions of various tissues. Since the histochemical methods are non-disruptive, the nucleic acid-protein responses could be related to cytomorphologic manifestations of cytopathology. Also, removal of various representative tissues from each animal, enabled the evaluation of cardiovascular responses in relation to the pathophysiological state of other organ systems within the same individual animal. In effect, the analytical approach used constitutes a "within animal assay" of nucleic acid response patterns where each rat serves as its own control with respect to analyses and interpretations of organ-system interactions following acute intoxication.

(2) Background

Current concepts of the physiopharmacological mode of toxicant action of trichothecene mycotoxins all implicate a direct binding to and interference with the synthesis of macromolecules. For example, it has been postulated that the inhibition of peptide synthesis stems in large part from an impairment in both the initiation and termination reactions of the ribosomal-protein synthetic cycle (1,2). Trichothecenes also inhibit DNA synthesis, and there have been sporadic reports that mycotoxins may exert mutagenic effects; however, very little detailed information is currently available regarding the mechanism involved in suppression of DNA synthesis or on the potential mutagenicity of mycotoxins *in vivo*.

It should be noted that to date most of the information relating to purported modes of action of mycotoxins at the cellular level is based on *in vitro* model systems. *In vitro* cultures of eukaryotic cell systems have received extensive use and have proven especially valuable in screening of toxin producing fungi, fractionation of toxicants from fungal metabolites and evaluation of comparative toxicities of chemically related analogues. On the other hand, the *in vitro* approach has not proven as fruitful in yielding precise information which can be extrapolated to the *in vivo* state, i.e., providing predictive data relating to the sequence of metabolic and cytopathic responses of the intact organism to T-2 toxin. The reason for this is clear. In *in vitro* systems, toxicity is limited solely by membrane solubility of the mycotoxin and the susceptibility of the cultured cells. Factors such as detoxification or biotransformation into more highly toxic forms, regional and systemic variations in delivery of toxic metabolites, and compensatory metabolic responses occurring at cellular or organismal levels can only be studied using *in vivo* approaches. At present, however, very scant information is available regarding *in vivo* metabolic and cytopathic responses of various organ systems of T-2 toxin.

Within the past several years, a number of experiments were conducted in our laboratories involving *in vivo* studies of metabolic responses of various tissues of rats exposed to the

trichothecene T-2 toxin. The central objective of these studies was to obtain more definitive information relating to acute T-2 toxin-induced changes in DNA, RNA, and protein metabolism in cardiovascular, hemopoietic, gastrointestinal, hepatic, renal and neural tissue compartments. Specific aims of these feasibility studies were to: 1) chararacterize in more detail the precise nature of alterations in transcriptional-translational capabilities of various organ-systems in vivo; 2) identify specific cell types undergoing metabolic transformation and incipient degeneration; and 3) relate dose-dependent metabolic responses to cytopathic or overt manifestations of toxicity.

In addition to documenting the feasibility of using microscopic cytophotometric procedures in toxicological studies of the cellular mode of action T-2 toxin, evidence was obtained supporting the existence of injury to both nuclear and cytoplasmic (ribosomal) components of myocardial cells.

Although there have been numerous reports relating to systemic effects of T-2 toxin and other trichothecenes, most of these simply document the presence of lesions or histopathological alterations in various organs. No studies were found which involved use of qualitative and/or quantitative histochemical analyses of nucleic acid-protein response patterns in various target sites of T-2 toxicant action. Also, the nature and time-course of acute and subacute effects of T-2 toxin on such organs as the heart, liver, kidney and brain are poorly documented (3).

It is generally conceded that irrespective of route of administration (oral, topical, parenteral), T-2 toxin is rapidly disseminated throughout the body with highest concentrations found in the liver and kidney within hours after toxin challenge. Most workers also are in agreement that in vivo as in vitro the initial biochemical lesion is an inhibition of cellular protein synthesis involving T-2 toxin binding to ribosomes and blockage of peptidyl transferase activity, the key step involved in the initiation phase of protein synthesis (1,2). The widespread toxic effects observed in vivo, including necrosis in enteric, hepatic and other body compartments are presumed to be directly related to T-2 toxin inhibition of protein synthesis and subsequent impairment in RNA synthesis. However, supportive evidence that this is what occurs in vivo is lacking since, to date, most studies focusing on the cellular mode of trichothecene toxin action have involved use of cell culture model systems.

In view of the foregoing considerations, the research described in the present report was designed to obtain more definitive confirmation that in vivo as in vitro the primary biochemical lesion underlying cytotoxic and lethal actions of T-2 toxin is an impairment in regulatory aspects of protein and nucleic acid biosynthesis. An equally important aspect of the experimental design focused on quantification of nucleic-protein response patterns in several putative organs (i.e.,

brain, heart, liver and adrenal glands) which have not been extensively studied by previous workers.

(3) Rationale Used in Current Study

A major impetus for initiating the current study was the availability of requisite instrumentation and capability for quantifying nucleic acid-protein responses in several vital organ-system compartments in animals treated with T-2 toxin. This approach thus enabled the testing of several hypotheses relating to the cellular mode of action of T-2 toxin.

For example, one hypothesis holds that in vivo as in vitro the initial biochemical event which precipitates cytotoxicity is an inhibition of protein synthesis and RNA depletion in a secondary effect resulting from an impairment in regulatory mechanisms of macromolecular metabolism. The research strategy used to test this hypothesis, and also to identify primary versus secondary target sites of T-2 toxin action, entailed use of cytophotometric measures of DNA, RNA and protein response patterns in various tissue compartments. Evidence is presented that supports this hypothesis, at least with respect to target sites such as the heart.

A second hypothesis formulated at the onset of the research was that an important aspect of acute T-2 toxin poisoning involves the release of vasoactive substances such as histamine, thereby contributing to vasodilatation, hypotension and blood stasis. This also was validated by cytophotometric analyses of mesenteric mast cell granulation and biochemical assay of circulating plasma histamine concentration; both responses proved to be dose-dependent in T-2 toxin treated rats .

Selection of the specific cytochemical nucleic acid probes which were used, i.e., Feulgen-DNA†, and azure B-RNA†, was based on the fact that these have been extensively validated and widely used in a variety of studies of transcriptional-translational aspects of metabolic alterations associated with normal developmental as well as various disease processes (4,5). Scanning-integrating microdensitometry† was adopted as the major analytical method since this constitutes among the most sensitive techniques currently available for quantification of alterations (in picogram or femtogram levels) of organic constituents on an individual cell basis with no disruption of the histomorphological integrity of tissues being analyzed.

Parallel microchemical analysis of T-2 toxin induced alterations in nucleic acids in relation to morphological manifestations of histopathology is especially useful for several reasons. It allows comparisons to be made of the time course of biosynthesis of macromolecules at the cellular level in relation to vascular injury mediated-inflammatory responses within various target tissue compartments in the same animal. Furthermore, it permits more

meaningful interpretations relating to the cellular mode of toxin action in precipitating impairments in regulatory aspects of DNA-template and/or ribosomal-protein synthetic activities in relation to vascular injury mediated-inflammatory reactions.

An equally important reason for undertaking the present study was the recognition that there is no specific prophylaxis or therapy of trichothecene poisoning which is effective. This stems in large part from the multi-organ pathology which occurs with trichothecene intoxication and insufficient information on primary versus secondary target sites of toxicant action. It was felt that the use of microchemical probes in assessing the severity of T-2 toxin-induced impairment in macromolecular synthesis in known and putative target sites would provide useful information relating to systemic changes which ultimately precipitate cardiovascular shock. Such information is essential for rational decision making in the development of appropriate drugs for enhanced protection beyond that provided by current methods of medical defnese against trichothecene toxic agents.

(4) Experimental Methods

Adult male Sprague-Dawley rats (Hilltop Labs) weighing 200-220 g were used for in vivo studies of acute (8-12 h) and delayed (1 to 3 wks) effects of a single intraperitoneally (ip)† administered injection of purified T-2 toxin (Sigma). A total of 240 rats was used in six separate experimental runs focusing on quantitative nucleic acid-protein responses in cardiovascular, neural, hepatic, lymphoidal and enteric tissue compartments. A wide range of dosages was used, i.e., sublethal (0.5-0.75 mg/kg), near-lethal (0.9-1.5 mg/kg) and lethal (6 mg/kg) doses prepared in ethanol and injected in a final volume of 0.5 ml/kg body weight; the LD_{50}† dose was predetermined to be 0.9 mg/kg by body weight. Specific doses, numbers of animals in different treatment groups are presented in appropriate tables in the Results section for various tissues which were analyzed.

In all experiments, an assembly line procedure involving participation of 6-8 individuals was employed to expedite removal and fixation of tissues immediately after decapitation, i.e., within three min. of the designated kill time. Basically, the tissue processing and staining protocol was as follows:

Rats were killed by decapitation at designated times and various tissues removed, cut into smaller pieces and fixed in 10% neutral buffered formalin at 4C for 24 h; these were paraffin processed and serially sectioned using a calibrated microtome. The following tissues were obtained from 5-6 representative rats per treatment group: heart, brain, spleen, thymus, small intestine, cecum, liver, kidney, adrenal and mesentery.

Several types of staining procedures were used: 1) conventional differential staining using hematoxylin-eosin (H & E)†

Papanicolaou or Mallory triple stain for analyses of cytomorphological alterations; 2) analytical stoichiometric staining for subsequent quantification of macromolecular changes, i.e., the Feulgen nucleal reaction† for chromatin and DNA changes (6,7); the azure B reaction for RNA (8,9); and the Coomassie brilliant blue† reaction for total protein (9,10,11). Specificity of nucleic acid staining was confirmed using control sections treated with DNase† with and without RNase† prior to azure B-RNA or Feulgen DNA staining.

Cytophotometric analyses of cellular chromatin, RNA and protein content in known and putative target sites of T2 toxicant action were made using a Vickers M85a scanning-integrating microdensitometer (Vickers Instruments, Malden, MA) as described previously (7,9). A variable field delimiting mask aperture was used to isolate and delimit individual cells being analyzed. Measurements were made at a magnification of 1000X at the absorption maximum of Feulgen-DNA (540 nm), azure B-RNA (580 nm) or Coomassie protein (595 nm). It was ascertained that the extent of error in nucleic acid-protein measurements attributable to differences in section thickness (<2%) or instrument performance (<1%) is negligible relative to the normal extent of intercellular variability (ca. 20-30%) in levels of RNA and protein in tissues under analysis.

Correlative data were also obtained on dose-dependent alterations in circulating plasma histamine levels in T-2 toxin treated rats at 8 h post-injection using the enzymatic-isotopic microassay of Taylor and Snyder (12) as modified by Shaff and Beaven (13). Briefly, this histamine assay is based on the methylation of histamine by added histamine methyl-transferase (HMT) and [^{3}H]-labelled S-adenosyl-L-methionine, [^{3}H]SAMe (New England Nuclear), in the presence of cofactor pyridoxyl-5'-phosphate (Sigma). Because the methylation of tissue histamine to N-methylhistamine is uniform, one can readily measure nanogram levels of histamine after separation of the [^{3}H] methylhistamine from [^{3}H]SAMe by extraction into a 20% isoamyl alcohol/80% toluene mixture, adding the extract to scintillation vials with Formula 963 (New England Nuclear) and counting using a liquid scintillation counter (Tri-Carb 406C, Packard Instr. Co., Downers Grove, IL). Similar enzymatic-isotopic analyses of histamine levels were made using homogenates of lung and cecum tissue.

To obtain an independent assessment of T-2 toxin induced mobilization of vasoactive substances and relate this to plasma histamine levels, quantitative analyses of mesenteric mast cell degranulation were undertaken. This entailed use of metachromatic† staining of mesenteric spreads affixed to slides and the cytophotometric assay of Kelly and Bloom (14,15) to determine the extent to which the release of autacoids† by mast cells in loose connective tissue compartments follows a dose-dependent response pattern during acute T-2 toxin exposure.

Several in vitro experiments were also conducted using cultured bovine aortic endothelial cells (BAEC)† and smooth muscle cells (SMC)† exposed to T-2 toxin. The major focus of this facet of the overall study was to investigate the effects of T-2 toxin on RNA levels of BAEC using the pyronin Y-RNA flow cytofluorescence assay described by Shapiro (16). Briefly, this entailed the following methodology:

Endothelial cells were isolated from the thoracic aorta of mature bovine females. Aortas were aseptically excised from the animal immediately following slaughter, placed in ice-cold sterile Hank's Balanced Salt Solution (HBSS, Flow Laboratories, McLean, VA) with 100 U/ml penicillin-streptomycin (Flow Laboratories). After a rinse in sterile HBSS, the aortas were cleaned of adventitia and given a final rinse in calcium- and magnesium-free HBSS. One end of the aortic segment was clamped with large hemostats; the intercostals were closed with sterile seraphines. A volume of 0.1% collagenase-dispase (Boehringer-Mannheim Biochemicals, Indianapolis, IN) and 0.15% trypsin (Sigma Chemical Company, St. Louis, MO) in calcium- and magnesium-free HBSS sufficient to fill the lumenal space was pipetted through the open end of the aortic segment. The closed aorta was incubated for approximately 15 minutes at 37°C in 5% CO_2 and agitated by gentle rolling during this period. The aorta was opened and the resultant cell suspension was pipetted in 10 ml aliquots to 15 ml centrifuge tubes containing 5 ml Minimum Essential Medium (MEM, Flow Laboratories) supplemented with 10% fetal bovine serum (Sterile Systems, Logan, UT) to inhibit further proteolytic activity. Each tube was centrifuged for 5 minutes, the supernatant discarded, the pellet resuspended in the serum-supplemented MEM and plated at 50,000 cells/ml in 75 cm^2 tissue culture flasks (Costar, Cambridge, MA). Cultures were then incubated with 5% CO_2 in air and grown to confluency.

Bovine aortic smooth muscle cells were the generous gift of Drs. Patricia D'Amore and Alicia Orlidge of Children's Hospital, Boston.

Endothelial and smooth muscle cells were plated at a seeding density of 20,000 cells/cm^2 in 25 cm^2 tissue culture flasks and grown in MEM supplemented with 10% serum. Cultures of both cell types were grown to an approximately confluent state at which point test reagents were added to the culture medium.

Pyronin Y† staining and flow cytometric analysis were conducted using the method described by Shapiro (16). Briefly, cells were removed from the culture vessel by treatment with 0.15% trypsin in HBSS, washed, suspended in 1 ml MEM, and fixed with the dropwise addition of 100% ethanol in equal volume. Fixed cells were then washed and resuspended in HBSS. Appropriate samples were treated for 30 min at 37°C with 6.25 U/ml RNase (Boehringer-Mannheim). Pyronin Y at a final concentration of 5 uM was then added to all samples which were kept on ice for 45 minutes before flow cytometry.

Statistical analyses of data were performed using analysis of variance (ANOVA), Duncan's multiple range test and the heterogeneous χ^2 test. When the ANOVA F-test revealed significant differences between group means, the data were further analyzed using Duncan's test. In addition, individual RNA and protein values were examined in conventional frequency distribution profile form. Histograms were constructed to demonstrate the frequency occurrence of neurons containing low, moderate and high RNA and protein levels, with the moderate category arbitrarily designated as that portion of the neuronal population where individual RNA and protein values fall within the range of ethanol-control mean ±1.0 standard deviation; low and high RNA and protein categories thus represent neurons with measured values for these cytochemical parameters which were less or greater than one deviation from the respective control mean value. Differences among distribution profiles were then compared using the heterogeneous χ^2 test. In all analyses, probabilities of 5% were interpreted as statistically significant.

(5) Results

To facilitate presentation, the overall results from various subprojects are summarized under four headings entitled: I. Cardiovascular Effects of T-2 Toxin; II. Neurotoxic Effects of T-2 Toxin; and III. Other Systemic Effects of T-2 Toxin. Also, in instances where data have been published or are in press, brief summaries of major findings and conclusions are presented with appropriate references to specific publications containing supportive documentation.

I. Cardiovascular Effects of T-2 Toxin

1. Overt and Microscopic Manifestations of Cardiotoxicity

A consistent feature of acute T-2 toxin poisoning at necropsy was a prominent venous congestion in visceral organs and mesenteries in rats sacrificed at 8 h post-injection. As anticipated, the extent of congestion was more severe in the higher dosage treatment groups (1.5 and 6 mg/kg). In the 6 mg/kg group rats were killed when they showed signs of respiratory collapse and impending death (5-6 h); these typically exhibited gross hemorrhagic ulcerations on the serosal surface of the small and large intestine and blood in the intestinal lumen. Several rats receiving lethal doses of T-2 toxin also exhibited focal hemorrhages in the heart and lung.

Microscopic analysis of differentially stained myocardial sections revealed the presence of interstitial edema notably in the endocardial region. This was manifested in a separation of muscle fascicles and a widening of the subendothelial compartment by clear acellular spaces. The extent of myocardial edema was most severe in rats exposed to the highest dosage (6 mg/kg) and was associated with focal regions of sarcolysis, i.e., reduced basophilic† staining and "cloudy swelling" appearance of sarcoplasm. There was no evidence of lymphocytic infiltration into the interstitial compartment. Coronary blood vessels were typically engorged with a widening of adventitial spaces; again this was most severe in the higher dosage groups indicative of endothelial injury, increased permeability and extravasation of plasma into the interstitium. In rats given a 0.9 LD_{50} dose which were killed seven days later, Mallory stained sections revealed an hyperchromaticity of muscle fascicles bordering the tunica intima; however, the extent of interstitial edema was less pronounced than was observed during the acute (8 h) post-injection interval in rats injected with near-lethal (1.0-1.5 LD_{50}) doses of T-2 toxin. Nuclear manifestations of cardiotoxicity which were visually discernible included nuclear hypertrophy and chromatin condensation†. Again, nuclear chromatin alterations were more pronounced with near-lethal and lethal dosages.

2. Cytophotometric Analyses of Chromatin and Macromolecular Changes

Among the parameters used to quantify T-2 toxin-induced cardiotoxicity included: (a) nuclear area and photometric area as an indicator of nuclear size changes and of chromatin dispersion†; (b) Feulgen DNA levels and shifts in relative abundance of myocardial cells exhibiting low and high affinities for nuclear F-DNA staining(F-DNA reactivity)†; (c) myocardial RNA levels; and (d) myocardial protein levels. Tabular and graphic summaries of data are presented in Tables 1-4 and Figures 1-3.

Major findings supported by these data are as follows:

(a) Acute T-2 toxicity is associated with a dose-dependent myocardial nuclear hypertrophy. This is reflected in an increase in both nuclear size, notably in 1.5 and 6.0 mg/kg treatment groups measured using ocular filar micrometry; also, in the area of the nucleus containing F-DNA chromophore† measured cytophotometrically (Table 1). The latter finding indicates a dispersion of F-DNA stained chromatin.

(b) Average myocardial nuclear F-DNA levels expressed in absorbancy units (A.U.)† are generally maintained within the control range with the 6.0 mg/kg group exhibiting a 11% decrease in F-DNA and the 0.9 mg/kg group sacrificed at 7 d post-treatment exhibiting a 12.7% decrease in F-DNA levels relative to controls (Table 2).

Table 1: Effect of T-2 Toxin on Myocardial Nuclear Chromophore Area and Nuclear Envelope Area.

Treatment Group T-2 Toxin Dosage	Micrometer Area[a]	Δ%	Photometric Area[b]	Δ%
Ethanol Control	97.3 + 1.9[3]		61.8 + 0.2[3]	
T-2 toxin 0.83 LD_{50} (0.75 mg/kg)	100.2 + 2.1[3]	+3.0	59.6 + 0.2[3]	-5.1
T-2 toxin 1.1 LD_{50} (1.0 mg.kg)	98.3 + 2.2[3]	+1.5	67.2 + 0.2[2]	+8.9
T-2 toxin 1.67 LD_{50} (1.5 mg/kg)	110.7 + 3.1[2]	+13.8	73.6 + 0.2[1]	+17.2
T-2 toxin 6.67 LD_{50} (6.0 mg/kg)	115.8 + 3.1[1]	+19.0	73.8 + 0.3[1]	+17.5
T-2 toxin 1.0 LD_{50} (0.9 mg/kg, 7 d delay)	98.3 + 2.8[3]	+1.0	66.6 + 0.2[2]	+6.0

[a]Area of nuclear envelope (μm^2 + Standard Error) determined using calibrated ocular filar micrometry. A total of 100 individual nuclear measurements were made per group.

[b]F-DNA chromophore area (μm^2 + Standard Error) determined using scanning-integrating microdensitometry. A total of 120 individual nuclear measurements were made per group. Means with different superscripts are significant, $p < 0.05$, Duncan's multiple range test.

Table 2: Effect of T-2 Toxin on Myocardial Cell Feulgen-DNA Levels.

Treatment Group T-2 Toxin Dosage	N(n)[a]	Myocardial Nuclei[b] A.U. + S.E.	C.V.	%Δ
Ethanol Control	6(117)	32.9 ± 0.3[1]	10.7	
T-2 toxin 0.83 LD_{50} (0.75 mg.kg)	6(113)	31.1 ± 0.4[1]	14.4	-5.5
T-2 toxin 1.1 LD_{50} (1.0 mg/kg)	6(107)	32.3 ± 0.4[1]	12.5	-1.8
T-2 toxin 1.67 LD_{50} (1.5 mg/kg)	7(109)	31.6 ± 0.4[1]	13.5	-3.8
T-2 toxin 6.67 LD_{50} (6.0 mg/kg)	6(118)	29.2 ± 0.5[2]	18.3	-11.0
T-2 toxin 1.0 LD_{50} (0.9 mg/kg, 7d delay)	7(134)	28.7 ± 0.4[2]	17.7	-12.7

[a]N, Number of animals per treatment group; n, number of individual cell measurements

[b]Mean ± Standard Deviation (Standard Error) in Absorbancy Units (A.U.); means with different superscripts are significant, $p < 0.05$, Duncan's multiple range test.

Table 3: Effect of T-2 Toxin on Myocardial Cell Azure B-RNA Content.

T-2 Toxin Dosage	N(n)[a]	Myocardial RNA[b] A.U. S.E.	C.V.	%Δ
Ethanol Control	6(120)	30.5 ± 0.6[1]	22.5	
T-2 toxin 0.83 LD_{50} (0.75 mg/kg)	6(120)	25.1 ± 0.5[2]	21.2	-17.5
T-2 toxin 1.1 LD_{50} (1.0 mg/kg)	6(120)	27.0 ± 0.6[2]	24.4	-11.4
T-2 toxin 1.67 LD_{50} (1.5 mg/kg)	7(120)	27.6 ± 0.6[2]	23.4	- 9.5
T-2 toxin 6.67 LD_{50} (6.0 mg/kg)	6(120)	22.3 ± 0.6[3]	26.9	-27.0
T-2 toxin 1.0 LD_{50} (0.9 mg/kg, 7d delay)	7(140)	26.5 ± 0.7[2]	29.2	-13.1

[a]N, number of animals per treatment group; n, number of individual cell measurements

[b]Mean ± Standard Error in Absorbancy Units (A.U.); coefficient of variation (C.V.) and percentage change relative to control level (%Δ); means with different superscripts are significant, $p < 0.05$, Duncan's multiple range test.

Table 4: Effect of T-2 Toxin on Myocardial Cell Protein Content.

T-2 Toxin Dosage	N(n)[a]	Myocardial Protein[b] A.U. S.E.	C.V.	%Δ
Ethanol Control	6(100)	47.2 ± 0.7^{1}	15.8	
T-2 toxin 0.83 LD_{50} (0.75 mg/kg)	6(100)	37.1 ± 0.5^{2}	12.9	-21.5
T-2 toxin 1.1 LD_{50} (1.0 mg/kg)	6(100)	31.2 ± 0.5^{3}	14.7	-34.0
T-2 toxin 1.67 LD_{50} (1.5 mg/kg)	7(100)	31.5 ± 0.4^{3}	10.5	-33.3
T-2 toxin 6.67 LD_{50} (6.0 mg/kg)	6(100)	27.7 ± 0.5^{4}	18.5	-41.3
T-2 toxin 1.0 LD_{50} (0.9 mg/kg, 7d delay)	7(100)	37.0 ± 0.6^{2}	16.0	-21.7

[a]N, Number of animals per treatment group; n, number of individual cell measurements

[b]Mean ± Standard Error in Absorbancy Units (A.U.); coefficient of variation (C.V.) and percent change relative to control level (%Δ); means with different superscripts are significant, $p < 0.05$, Duncan's multiple range test.

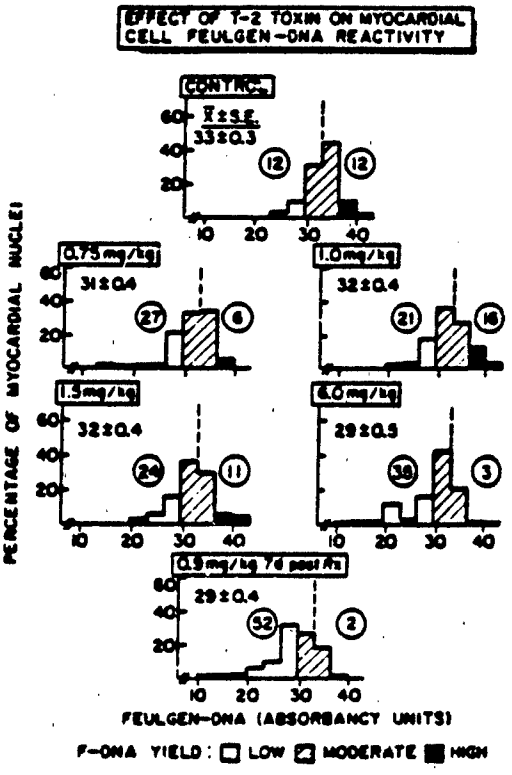

Fig. 1. Frequency Distribution Profiles Depicting T-2 Toxin-Induced Alteration in Myocardial Cellular Chromatin Feulgen-DNA Levels (8 hr postexposure). Measurements were made at 540 nm. Histograms were constructed to demonstrate the frequency occurrence of nuclei exhibiting low, moderate and high F-DNA yield; the moderate category represents that portion of the cell population where ndividual F-DNA values fall within ± one standard deviationof the mean. Circled numbers indicate percentages of corresponding low or high F-DNA categories. Reproducibility of individual nuclear DNA measurements was ±2%.

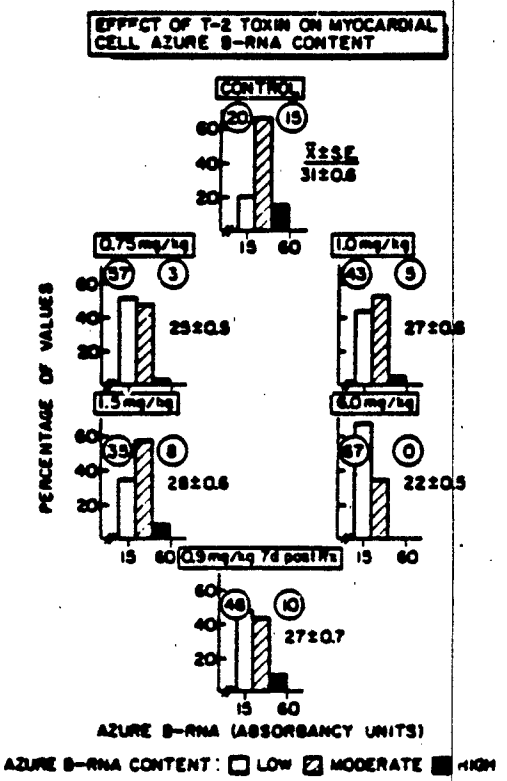

Fig. 2. Frequency Distribution Profiles of Azure B-RNA Contents of Myocardial Cells of Acute T-2 Toxin-Treated Rats (8 hr postexposure). Low and high categories (circled numbers) represent the percentage of cells whose RNA contents areless or greater than one standard deviation from the mean control value.

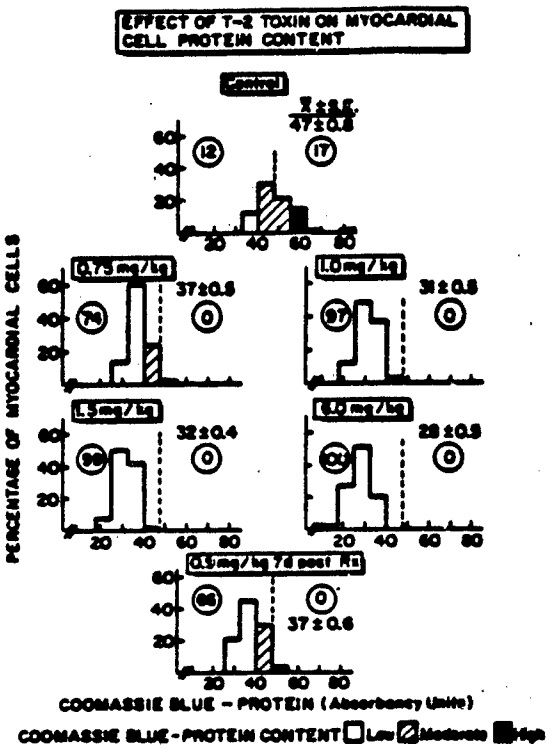

Fig. 3. Frequency Distribution Profiles of T-2 Toxin-Induced Alterations in Myocardial Cellular Protein Levels (8 hr postexposure). Low and high Coomassie blue-protein categories (circled numbers) represent the percentages of cells whose protein contents are less or greater than one standard deviation from the mean control value.

(c) There is a marked increase in the relative abundance of myocardial cells exhibiting low F-DNA reactivity† (Fig. 1). This is evidenced even with sublethal dosages of 0.75 and 1.0 mg/kg at 8 h post-injection and is especially marked in the 0.9 mg/kg treatment group sacrificed 7 d post-treatment.

(d) A depletion in both myocardial RNA levels (Table 3, Fig. 2) and in protein levels (Table 4, Fig. 3) is evidenced with both sublethal and lethal dosages of T-2 toxin. Because of the high coefficient of variation in RNA (21-29%) and protein (11-16%) levels, this is more clearly reflected from analyses of histogram profiles which reveal a several fold increase in the abundance of low RNA and a virtually complete absence of moderate and high protein containing cardiocytes in rats injected with sublethal and lethal levels of T-2 toxin.

3. Plasma Histamine Levels and Mesenteric Mast Cell Degranulation

Data relating to the effects of sublethal and lethal levels of T-2 toxin on plasma, cecal and lung histamine levels are summarized in Table 5. A dose-dependent elevation in circulating plasma levels was evidenced with the 1.0 and 1.5 mg/kg groups exhibiting approximately two- and three-fold increases, respectively, over basal ethanol injected control levels. Enteric histamine levels tended to be higher in T-2 toxin treated rats but did not prove to be statistically significant owing to the high variance and small number of rats per treatment group. However, if one combines data from the four T-2 toxin rats irrespective of dosage the overall mean histamine level of 2.84 ± 0.5 is approximately 80% over that of controls ($p < 0.05$). Basal control levels of lung histamine levels were appreciably higher than cecal levels and were not affected by T-2 toxicant exposure.

In a related study the effects of T-2 toxin on mesenteric mast cell degranulation were determined using scanning microdensitometric analyses of individual cellular metachromasia†. Based on data summarized in Table 6, it is clear that there is an increase in mast cell depletion indicative of the release of histamine and perhaps other vasoactive substances mediated by T-2 toxin action.

4. In vitro Studies of T-2 Toxin Effects on RNA and Protein Levels of Cultured Endothelial Cells.

In preliminary experiments, a differential susceptibility of cultured bovine smooth muscle cells (SMC) and aortic endothelial cells (BAEC) to T-2 cytotoxicity was noted. For example, T-2 concentrations of up to 10 ug/ml failed to elicit morphologically detectable cytopathic changes in SMC. Endothelial cultures, on the other hand, failed to remain viable during 12 hour incubations with T-2 toxin concentrations as low as 50 ng/ml. In light of the observed dramatic effects of T-2 toxin on the vascular system in vivo and its established affinity for polyribosomal RNA, these preliminary findings indicating a high endothelial cell susceptibility to T-2 toxin in vitro, in part, prompted

Table 5: Effect of T-2 Toxin on Plasma, Enteric and Lung Histamine Levels

Treatment Group		Histamine Levels ± S.E.[b]		
T-2 Toxin Dosage	N[a]	Plasma ng/ml	Gut ng/mg protein	Lung ng/mg protein
Ethanol Control	6	75.7± 9.6[4]	1.58±0.22[2]	26.5±5.4[1,2]
0.5 mg/kg	6	86.7± 7.1[3,4]	3.60±1.09[1]	36.4±5.8[1]
0.75 mg/kg	6	111.0±24.9[3]	3.28±0.77[1]	24.5±2.7[2]
1.0 mg/kg	7	170.6±36.7[2]	1.83±0.74[1,2]	26.1±4.1[1,2]
1.5 mg/kg	7	229.0±23.0[1]	1.62±0.34[2]	26.2±2.0[1,2]

[a]N designates number of animals per treatment group

[b]Average histamine levels ± standard error assayed using the enzymatic-isotopic method of Taylor and Snyder (12); means with different superscripts are significant, $p < 0.05$, Duncan's multiple range test.

Table 6: Mesenteric Mast Cell Degranulation in Acute T-2 Toxin Treated Rats[a]

T-2 Toxin Dosage	N(n)	Mast Cell Metachromasia[b] (A.U.±S.D.)	%Δ
Control	6(120)	165±65[1]	
0.5 mg/kg	6(120)	127±37[4]	-23
0.75 mg/kg	6(120)	134±25[3,4]	-19
1.0 mg/kg	6(120)	150±26[2]	- 9
1.5 mg/kg	6(120)	142±24[2,3]	-14

[a]Extent of mast cell degranulation based on scanning microdensitometric measures of metachromatic dye binding of cytoplasmic granules using azure B-stained mesenteric spread preparations. N(n) designate number of rats and number of individual mast cells measured.

[b]Average levels expressed in Absorbancy Units (A.U.) ± Standard Deviation. Means with different superscripts are significant, $p < 0.05$, Duncan's multiple range test. Percentage change (Δ%) relative to ethanol injected controls.

us to examine specific effects of T-2 toxicant actions on RNA content in cultured BAEC.

Flow cytometric analysis of Pyronin Y-stained endothelial cells yielded strong evidence evidence of T-2 toxicant action in this cell type (Table 7). Treatment of fixed BAEC with 6.25 U/ml RNAse reduced peak channel fluorescence 30% with respect to untreated aliquots. BAEC cultures exposed to 5 ng/ml T-2 toxin for 12 hours prior to analysis exhibited a 20% decrease in peak fluorescence. This represents an approximately 68% reduction in Pyronin Y fluorescence attributable to specific RNA binding. Exposure of BAEC to T-2 toxin also decreased the ability of RNase treatment to diminish Pyronin Y fluorescence (40%). Peak fluorescence in this group was 17.9% lower than the untreated control. The results of this study clearly indicate that exposure to even minute quantities of T-2 toxin decreases Pyronin Y-RNA fluorescence in fixed BAEC.

An independent assessment of T-2 toxin induced effects on total azurophilia† and RNA content was conducted using azure B stained BAEC cultures on coverslips. Based on data summarized in Table 8 it is clear that T-2 toxin exhibits a marked dose-dependent depletion in azurophilic staining and in azure B-RNA levels.

5. Cytointerferometric Analyses of Protein Changes in Endothelial Cells

Time constraints precluded the undertaking of extensive use of microinterferometry† in analyses of cytopathic responses in various target tissues of T-2 toxin exposed rats. Nonetheless, unstained sections of cardiac, enteric and other organs; also, "en-face"† preparations of cardiovascular endothelial cells; and monolayers of cultured endothelial cells are currently being analyzed to obtain supplemental data specifically relating to cellular protein responses associated with acute T-2 mycotoxin poisoning. To date, preliminary analyses (data not presented) provide supportive evidence that T-2 toxin exerts a direct cytotoxic action on endothelial cells with protein depletion constituting the initial cytopathic event which precedes inhibition of RNA synthesis and the suppression of chromatin template activity.

II. Neurotoxic Effects of T-2 Toxin

In vivo cytophotometric analyses were also conducted on brain specimens from the same groups of rats used in studies of cardiotoxic effects of T-2 toxin. The focus of this aspect of the study was on quantification of neuronal chromatin (F-DNA), azure B-RNA and Coomassie (caudate nucleus plus putamen) brain compartments. These brain regions were selected because of their role in locomotor control and hypokinesia is an early manifestation of T-2 toxin-induced CNS† dysfunction. Since two papers on neurotoxic effects of T-2 toxin are in press (7,9), brief summaries of major findings and conclusions are presented below.

Table 7: Effects of T-2 Toxin on PY-fluorescence of Cultured Aortic Endothelial Cells and Smooth Muscle Cells

Treatment Group	Staining Conditions	Cell Type	Peak Channel Fluorescence	Δ%	Mean Fluorescence	Δ%
Control	PY	BAEC	84		96.5	
Control	PY+RNase	BAEC	59	-30	74.7	-23
T-2 toxin	PY	BAEC	67	-20	81.9	-15
T-2 toxin	PY+RNase	BAEC	69	-18	91.7	- 5
Control	PY	SMC	-	-	126.5	
Control	PY+RNase	SMC	-	-	118.3	- 7
T-2 toxin	PY	SMC	-	-	110.6	-18
T-2 toxin	PY+RNase	SMC	-	-	112.9	-11

[a]Endothelial cells (BAEC) and smooth muscle cells (SMC) were plated at a seeding density of 20,000 cells/cm^2 in 25 cm^2 tissue culture flasks. Pyronin Y staining (PY) and flow cytometric analysis were conducted using the method of Shapiro (1981) with and without pretreatment with RNase (6.25 U/ml at 37 C for 30 min). There was no identifiable PY peak channel fluorescence obtained with SMC cultures. T-2 toxin dosage was 5 ng/ml for 12 h prior to analysis.

Table 8: Effects of T-2 Toxin on Total Azurophilia and Azure B-RNA Levels of Cultured Aortic Endothelial Cells

Treatment Group	n	Total Azurophilia A.U.±S.D.(S.E.)	%Δ	Azure B-RNA (A.U.±S.D.(S.E.)	%Δ
Control	100	64.1±15.9(1.6)		42.7±10.4(1.0)	
T-2 toxin (0.05 ng/ml)	100	35.0± 7.7(0.8)	-45	37.8± 6.9(0.7)	-11
T-2 toxin (5.0 ng/ml)	100	24.9± 5.7(0.6)	-61	19.5± 5.0(0.5)	-54

[a]Bovine aortic endothelial cells (BAEC) were plated at a seeding density of 20,000 cells/cm^2 in 25 cm^2 tissue culture flasks containing coverslips. Coverslips containing monolayers of BAEC were treated with DNase (for azure B-RNA) or untreated with DNase (for total azurophilia) prior to azure B staining and scanning-integrating microspectrophotometry; average values are expressed in absorbancy units (A.U.) ± standard deviation (standard error) and based on 100 individual cell measurements per treatment group. The designated T-2 toxin dosages were for 12 h prior to analysis.

1. Overt and microscopic manifestations of neurotoxicity Changes

The predominant overt CNS symptoms of T-2 intoxication included asthenia and hypokinesia and generally occurred about 4 h post-injection, whereas vascular changes such as episodic hyperemia of external ears were evidenced as early as 1 h after toxin injection. At the time of decapitation (8 h) rats receiving 0.75 to 1.5 mg/kg of T-2 toxin were lethargic but otherwise exhibited no overt signs of distress. The highest dosage group (6.0 mg/kg) exhibited signs hyporeflexia, prostration, coma and labored breathing at about 5-6 h after injections. At necropsy there was no evidence of brain hemorrhages; the method of euthanasia (decapitation) precluded assessment of the extent of meningeal vascular congestion.

Microscopic examination of H & E stained sections confirmed the absence of any focal brain hemorrhages. There was no discernible evidence of incipient necrosis. Neurons were normal in appearance with vesicular, euchromatic nuclei containing a strongly basophilic nucleolus with the soma containing moderate to abundant Nissl substance. On the other hand, perineuronal glial cell nuclei in T-2 poisoned rats exhibited some swelling with condensation of granular aggregates in the nucleoplasm.

2. Cytophotometric Analyses of Chromatin, RNA and Protein Changes

Comparison of average F-DNA levels of cerebrocortical (layer III) and striatal neurons in control and T-2 treated rats (Table 9) revealed dose-dependent diminutions in F-DNA reactivity of neurons in both brain regions, indicating a decrease in chromatin susceptibility to acid hydrolysis. Significant ($p < 0.05$) reductions in mean cerebrocortical neuron F-DNA reactivity ranged from 9% with 0.75 mg/kg to 22% with 6.0 mg/kg T-2, whereas the suppression in F-DNA reactivity in striatal neurons was slightly more severe, i.e., 15% with the lowest dose of T-2 and 26% with the highest. T-2 toxin-induced changes in neuronal F-DNA reactivity were further examined in conventional frequency distribution profile form (constructed using ethanol-control mean and standard deviation as the reference data base). Comparative analyses of F-DNA profiles indicated the existence of marked shifts in the relative proportions of nuclei n both cerebrocortical (layer III) and striatal neurons exhibiting low F-DNA yield. This was apparent in all T-2 toxin treatment groups as manifested by ca. 4-6 fold elevations in the frequency occurrence of low F-DNA categories. Thus, the existence of T-2 toxin-induced alterations in the physicochemical state of nuclear chromatin, i.e., its lability to Feulgen acid hydrolysis, was apparent not only in diminished mean F-DNA values (Table 9) but also in markedly elevated frequencies of ow F-DNA reactive nuclei with concomitant reductions in moderate and high F-DNA categories of the cortical and striatal neuron population.

Table 9: Comparative Analyses of Cerebrocortical (layer III) and Striatal Neuron Chromatin Feulgen-DNA (F-DNA) Reactivity in T-2 Toxin-Intoxicated Rats.[a]

T-2 Toxin Dosage	F-DNA Reactivity[b] Cortex	%Δ	Striatum	%Δ
Control	56.7 ± 4.6[1]		60.6 ± 7.4[1]	
0.75 mg/kg	51.9 ± 4.6[2]	- 8.5	51.8 ± 4.1[2]	-14.5
1.0 mg/kg	50.7 ± 5.5[2]	-10.6	50.2 ± 4.1[3]	-17.2
1.5 mg/kg	48.2 ± 5.4[3]	-15.0	48.8 ± 6.4[4]	-19.5
6.0 mg/kg	44.2 ± 7.5[4]	-22.0	45.2 ± 6.3[5]	-25.4

[a]T-2 toxin-induced alterations in neuronal F-DNA reactivity (Mean ± S.D.) based on scanning-integrating microdensitometric measures of dye binding using standardized hydrolysis protocol adopted for comparative analyses, i.e., 30 min in 3.5 N HCl at 37 C.

[b]Reaction product formation in Absorbancy Units (A.U.) ± Standard Deviation. Means with different superscripts are significant, $p < 0.05$, Duncan's multiple range test. Values ranked (1-5), the highest designated as (1). Measurements made at 540 nm, corrected for glare and residual distribution error. Reproducibility of individual nuclear DNA measurements was ±2%. Each value represents mean of 100 cytophotometric F-DNA determinations with 6 animals per group. Adventitial fibroblasts used as diploid reference cell standards yielded a mean of 60.6 ± 6.0 A.U. (n = 100)

To further explore the relationship between T-2 toxin intoxication and alterations in neuronal nuclear functioning, analyses of T-2 toxin-induced changes in the extent of chromatin compaction (F-DNA chromophore area) and of actual nuclear volume were conducted on the same series of sections used for determination of F-DNA reactivity responses. Based on the data presented in Table 10, photometric area, i.e., nuclear area containing F-DNA reactive chromatin, was significantly ($p < 0.05$) elevated in both cerebrocortical and striatal neurons with all four T-2 toxin dosages. It is also clear that T-2 toxin produced an increase in nuclear volume in both cerebrocortical and striatal neurons with all four T-2 dosages. It is also clear that T-2 produced an increase in nuclear volume in both cerebrocortical and striatal neurons. Neither response was, however, strictly dose-dependent.

Similar measures were made of nucleolar volume changes using ocular filar micrometry of azure B stained brain sections. Both cerebrocortical and striatal neuronal nucleoli exhibited either no change or a moderate nucleolar hypertrophy (ca. 16%) in the 6 mg/kg and 1.5 mg/kg T-2 treatment groups (Table 11). Also, average neuronal RNA levels in both brain regions of T-2 toxin-intoxicated rats generally remained within the control range (Table 12). However, a 17% reduction in mean neuronal RNA content was evidenced within the cerebral cortex with 1.5 mg/kg T-2 toxin, and a 20% loss in perikaryal RNA was observed within the striatum with 6.0 mg/kg.

T-2 mycotoxin-induced alterations in brain neuronal protein levels were much more pronounced than RNA changes. As indicated by data summarized in Table 12, T-2 toxin produced a severe, linear dose-dependent reduction in total neuronal protein content. Declines in mean values within the motor cortex ranged from 9% with 0.75 mg/kg to 46% with a 6.0 mg/kg toxin challenge. Neuronal protein loss was less marked in striatal than in cortical compartments, i.e., 20-25% diminutions with 1.0, 1.5 and 6.0 mg/kg, and no protein depletion whatsoever with 0.75 mg/kg T-2 toxin.

III. Other Systemic Effects of T-2 Toxin

Cytochemical and histopathological studies were also made of the liver, intestinal tract, adrenals, kidney, thymus and spleen. Although these are still in progress and constitute integral aspects of M.S. or honors research projects by several graduate students, sufficient data were generated within the last several months to enable an evaluation of the nature and severity of T-2 toxin-induced impairment in functioning of these organ-systems. These are summarized below.

1. Hepatotoxic Effects of T-2 Toxin

In addition to cytomorphology, three microchemical probes, i.e., Feulgen-DNA, azure B-RNA and Coomassie-protein, were used to analyze dose-dependent and time-dependent alterations in

Table 10: Comparative Analyses of Cerebrocortical (layer III) and Striatal Neuron Feulgen-DNA (F-DNA) Chromophore Area and Nuclear Volume in T-2 Toxin-Intoxicated Rats.

T-2 Toxin Dosage	F-DNA Chromophore Area (μm^2)[a]		Nuclear Volume (μm^3)[b]	
	Cortex	Striatum	Cortex	Striatum
Control	89.5±16.4[3]	84.4±12.1[3]	1016.0±273.2[3]	1100.0±217.0[4]
0.75 mg/kg	108.1±18.4[1]	101.3±12.3[1]	1196.4±361.5[2]	1196.1±219.4[3]
1.0 mg/kg	106.5±17.5[1]	99.7±18.3[1]	1146,1±152.5[2]	1409.0±337.0[1]
1.5 mg/kg	102.0±17,3[2]	95.5±13,2[2]	993.0±207.1[3]	1097.6±440.2[4]
6.0 mg/kg	98.4±13,9[2]	94.2±11.8[2]	1222.4±269.7[1]	1301.0±220.0[2]

[a]Photometric F-DNA chromophore area (mean ± standard deviation) determined using scanning-integrating microdensitometry. Relative photometric area units converted into absolute values by calibration with graded measuring apertures. Each value represents mean of 50 individual nuclear determinations. Means not designated with same superscript are significantly different, $p < 0.05$, Duncan's multiple range test. Values ranked (1-3), the highest designated as (1).

[b]Nuclear volume (mean ± standard deviation) determined at 1000X using calibrated ocular filar micrometry. Each value represents mean of 100 individual neuronal determinations. Nuclear volume calculated from $V = \Pi/6ab^2$, where a = diameter of major axis and b = diameter of minor axis. Means not designated with same superscript are significantly different, $p < 0.05$, Duncan's multiple range test. Values ranked (1-4), the highest designated as (1).

Table 11: Cerebrocortical (layer III) and Striatal Neuron Nucleolar Volumes in T-2 Toxin-Intoxicated Rats.[a]

T-2 Toxin Dosage	Nucleolar Volume (μm^3)	
	Cortex	Striatum
Control	15.9 ± 8.7[2]	13.8 ± 8.5[2]
0.75 mg/kg	16.5 ± 8.1[1,2]	15.0 ± 8.2[1,2]
1.0 mg/kg	18.0 ± 7.9[1,2]	16.3 ± 7.5[1,2]
1.5 mg/kg	18.0 ± 8.2[1,2]	16.5 ± 7.0[1]
6.0 mg/kg	18.6 ± 8.2[1]	15.5 ± 7.6[1,2]

[a]Nucleolar volumes (mean ± standard deviation) determined at 1000X using calibrated ocular filar micrometry. Each value represents mean of 100 individual neuronal determinations. Nucleolar volume calculated from $V = \pi/6D^3$, where D = diameter. Means not designated with same superscript are significantly different, $p < 0.05$, Duncan's multiple range test.

Table 12: Cerebrocortical (layer III) and Striatal Neuron RNA and Protein Contents in T-2 Toxin-Intoxicated Rats.[a]

T-2 Toxin Dosage	RNA Contents Cortex	Striatum
Control	72.3 ± 14.0[1]	43.6 ± 8.7[1]
0.75 mg/kg	76.4 ± 14.6[1]	42.4 ± 10.0[1]
1.0 mg/kg	73.8 ± 11.3[1]	40.4 ± 11.9[1]
1.5 mg/kg	60.0 ± 11.6[3]	43.5 ± 11.5[1]
6.0 mg/kg	68.6 ± 14.7[2]	34.9 ± 11.1[2]

T-2 Toxin Dosage	Protein Contents Cortex	Striatum
Control	75.3 ± 23.1[1]	43.7 ± 10.0[1]
0.75 mg/kg	68.4 ± 19.4[2]	44.7 ± 10.0[1]
1.0 mg/kg	62.9 ± 23.4[3]	35.0 ± 10.1[2]
1.5 mg/kg	58.8 ± 13.8[3]	33.0 ± 4.9[2]
6.0 mg/kg	41.1 ± 10.7[4]	33.4 ± 5.5[2]

[a]Neuronal azure B-RNA and Coomassie-protein contents (Absorbancy Units ± S.D.) determined using scanning-integrating microdensitometry. Each value represents mean of 100 individual neuron measurements Means not designated with same superscript are significantly different, $p < 0.05$, Duncan's multiple range test.

transcriptional-translational aspects of nucleic acid and protein metabolism in liver parenchymal cells. Also, because the type and pattern of cytopathic changes observed during the acute (8 h) phase of intoxication proved to be similar to those obtained with non-specific stress stimuli or other xenobiotics (drugs, toxins, etc.), the focus of this subproject was on delayed liver responses at 7, 14 and 28 day intervals after T-2 toxin treatment. The major aim was to determine the extent to which T-2 toxin causes progressive irreversible hepatocellular injury. Because previous studies in our laboratory have shown that the predominant cell type in periportal (PP) region of liver lobules is tetraploid (4) with appreciable higher RNA levels than are found in diploid (2C) cells, which comprise the centrilobular (cc) compartment, separate analyses were conducted of T-2 toxin induced cytochemical responses in both PP and CL regions.

The most prominent signs of hepatocellular injury included loss of basophilic staining and focal areas of necrosis containing fibrocytic elements. Generally, most parenchymal cell nuclei retained their normal, euchromatic vesicular appearance. Visually, the extent of reduction in basophilia was more pronounced in CL than in PP regions at 8 h post-injection.

Cytophotometric analyses of dose and time-dependent alterations in Feulgen-DNA reactivity revealed a maintenance of average F-DNA levels within the control ± one standard deviation range in both PP and CL compartments (Table 13). Similarly, except for PP cells of rats killed 4 weeks after exposure which exhibited a reduction in total azurophilia and in azure B-RNA levels (Tables 14 and 15) with both sublethal and near-lethal dosages, there was no consistent pattern of azurophilic or RNA responses which could be related to dose or time after exposure. Analyses of Coomassie blue-protein levels in parenchymal cells also indicated the absence of any protein depletion in hepatocytes of T-2 toxin treated rats (Table 16).

2. Enterotoxic Effects of T-2 Toxin

This subproject was limited to the cytomorphological and histopathological assessment of T-2 toxin-induced effects on various tissue compartments of the small intestine in an attempt to identify specific cell types which are most prone to injury. In the following, major findings from two separate studies are summarized, one dealing with acute dose-dependent enterotoxic effects where all rats were killed at 8 h post-injection with sublethal and lethal doses of T-2 toxin (ip) and the second (designated as "time-dependent" study) focusing on the type and nature of intestinal cytopathic changes which occur prior to the onset of overt symptoms of intoxication, i.e., during the 2 to 8 hr interval after a lethal dose of T-2 toxin was administered. In both studies, particular attention was focused on vascular, muscular, leucocytic, secretory and stromal components.

Table 13: Nuclear Chromatin Feulgen-DNA (F-DNA) Reactivity of Periportal and Centrilobular Hepatocytes in T-2 Toxin-Treated Rats (7-28 d post-injection).

T-2 Toxin Dosage	N(n)[a]	F-DNA Reactivity[b] Periportal	%Δ	Centrilobular	%Δ
Ethanol Control	12(345)	43 ± 10[1]		26 ± 9[2]	
At 7 days:					
0.60 mg/kg	5(125)	36 ± 9[3,4]	-16	20 ± 6	-23
0.75 mg/kg	6(125)	41 ± 13[1,2]	- 5	24 ± 8	- 8
0.90 mg/kg	5(125)	35 ± 12[4]	-19	27 b 10[1,2]	+ 3
At 14 days:					
0.75 mg/kg	5(110)	41 ± 12[1,2]	- 5	28 ± 11[1,2]	+ 8
0.90 mg/kg	5(110)	40 ± 13[2]	- 7	28 ± 11[1,2]	+ 8
At 28 days:					
0.60 mg/kg	5(110)	41 ± 10[1,2]	- 5	24 ± 7	- 8
0.75 mg/kg	5(110)	43 ± 13[1,2]	0	29 ± 11[1]	+11
0.90 mg/kg	5(110)	38 ± 12[3,4]	-12	26 ± 12[2]	0

[a]N, number of animals per treatment group; n, number of individual cell measurements.

[b]Mean ± Standard Deviation in Absorbancy Unitz (A.U.); percentage change relative to control level (%Δ); values with different superscripts are significant at $p < 0.05$, Duncan's multiple range test with the highest value designated (1).

Table 14: Cellular Azurophilia (Basophilia) of Periportal and Centrilobular Hepatocytes in T-2 Toxin-Treated Rats (7-28 d post-injection).

T-2 Toxin Dosage	N(n)[a]	Cellular Azurophilia (A.U.±S.D.) Periportal	%Δ	Centrilobular	%Δ
Ethanol Control	12(150)	50 ± 14[1]		32 ± 14[2,3]	
At 7 days:					
0.60 mg/kg	5(50)	49 ± 18[1]	- 2	35 ± 12[2]	- 9
0.75 mg/kg	6(50)	46 ± 14[1]	- 8	32 ± 10[2,3]	0
0.90 mg/kg	5(50)	38 ± 13[2]	-24	27 ± 10[3]	-16
At 14 days:					
0.75 mg/kg	5(50)	35 ± 8[2,3]	-30	30 ± 10[2,3]	- 6
0.90 mg/kg	5(50)	49 ± 23[1]	- 2	49 ± 17[1]	+53
At 28 days:					
0.60 mg/kg	5(50)	32 ± 8[3,4]	-36	28 ± 10[3]	-12
0.75 mg/kg	5(50)	27 ± 8[4]	-46	18 ± 6[4]	-43
0.90 mg/kg	6(50)	37 ± 10[2,3]	-26	35 ± 11[2]	+ 9

[a]N, number of animals per treatment group; n, number of individual cell measurements.

[b]Mean ± Standard Deviation in Absorbancy Units (A.U.); percentage change relative to control level (%Δ); values with different superscripts are significant at $p < 0.05$, Duncan's multiple range test with the highest value designated (1).

Table 15: Azure B-RNA Content of Periportal and Centrilobular Hepatocytes in T-2 Toxin-Treated Rats (7 - 28 d post-injection).

T-2 Toxin Dosage	N(n)[a]	Azure B-RNA (A.U.±S.D.)[b] Periportal	%Δ	Centrilobular	%Δ
Ethanol Control	12(150)	34 ± 11[1]		23 ± 9[2,3]	
At 7 days:					
0.60 mg/kg	5(50)	30 ± 14[2]	-10	21 ± 7[3]	- 9
0.75 mg/kg	6(50)	36 ± 10[1]	+ 6	18 ± 10[1]	+22
0.90 mg/kg	5(50)	33 ± 11[1]	- 3	23 ± 10[2,3]	0
At 14 days:					
0.75 mg/kg	5(50)	29 ± 6[2]	-15	20 ± 6[3]	-13
0.90 mg/kg	5(50)	37 ± 16[1]	+ 9	28 ± 10[1]	+22
At 28 days:					
0.60 mg/kg	5(50)	26 ± 7[3]	-24	23 ± 6[2,3]	0
0.75 mg/kg	5(50)	28 ± 7[2]	-18	15 ± 7[4]	-35
0.90 mg/kg	6(50)	26 ± 7[3]	-24	25 ± 7[2]	+ 9

[a]N, number of animals per treatment group; n, number of individual cell measurements.

[b]Mean ± Standard Deviation in Absorbancy Units (A.U.); percentage change relative to control level (%Δ); values with different superscripts are significant at $p < 0.05$, Duncan's multiple range test with the highest value designated (1).

Table 16: Cellular Protein Content of Periportal and Centrilobular Hepatocytes in T-2 Toxin-Treated Rats (7-28 d post-injection).

T-2 Toxin Dosage	N(n)[a]	Protein Content (A.U.±S.D.)[b] Periportal	%Δ	Centrilobular	%Δ
Ethanol Control	12(150)	81 ± 12[1]		8 ± 14[1]	
At 7 days:					
0.60 mg/kg	5(50)	79 ± 11[1]	-2	83 ± 11[1]	- 6
0.75 mg/kg	6(50)	78 ± 12[1]	-4	80 ± 11[2]	- 9
0.90 mg/kg	5(50)	79 ± 10[1]	-2	79 ± 14[2]	-10
At 14 days:					
0.75 mg/kg	5(50)	76 ± 10[2]	-6	87 ± 11[1]	- 2
0.90 mg/kg	5(50)	81 ± 13[1]	0	87 ± 13[1]	- 2
At 28 days:					
0.60 mg/kg	5(50)	85 ± 11[1]	+5	82 ± 9[2]	- 7
0.75 mg/kg	5(50)	81 ± 14[1]	0	80 ± 11[2]	- 9
0.90 mg/kg	6(50)	81 ± 10[1]	0	82 ± 9[2]	- 7

[a]N, number of animals per treatment group; n, number of individual cell measurements.

[b]Mean ± Standard Deviation in Absorbancy Units (A.U.); percentage change relative to control level (%Δ); values with different superscripts are significant at $p < 0.05$, Duncan's multiple range test with the highest value designated (1).

(a) Dose-dependent cytopathic alterations

All T-2 dosages (e.g., 0.5, 0.75, 1.0 and 1.5 mg/kg) elicited histopathological alterations in intestinal tissue compartments at the 8 hr post-injection interval, with the severity of lesion formation and specific cell types involved depending on the dosage administered. With a sublethal dose of 0.5 mg/kg, the predominant histopathic alterations included serosal petechial hemorrhages, moderate edema of the submucosa with increase in average extracellular collagen fiber spacing (measured by ocular filar micrometry) decreased cytoplasmic acidophiliaf and presence of pycnotic fibroblasts and lymphocytes within the lamina propria and submucosa. Both submucosal and adventitial blood vessels exhibited nuclear chromatin condensation, disruption of nuclear membranes and nuclear vacuolization. Chromatin condensation was also evidenced in cryptal epithelial cells, whereas villus enterocytes appeared normal in appearance as did the smooth muscle cells of the tunica muscularis and muscularis mucosa. Interestingly, vascular cytopathic nuclear alterations appeared to primarily involve arterial components; the integrity of veins and lymphatics was unaffected.

With a higher sublethal dosage of 0.75 mg/kg a similar but more severe pattern of vascular and epithelial injury was evidenced coupled with a marked disruption of the integrity of lymphoidal elements. The incidence of serosal hemorrhage was increased; both crypt and villus epithelial cells exhibited nuclear chromatin condensation, karyorrhexis and absence of mitotic activity; Paneth cell lysis was observed in some regions. Submucosal edema was more extensive with infiltration by lymphocytes and neutrophils. Germinal centers of Peyers patches exhibited moderate to severe necrosis of lymphocytic elements although cortical lymphocytes appeared unaffected. Again, arterial vessels were more distorted with pycnotic nuclei and disrupted endothelium whereas lymphatic and venous elements were normal. Smooth muscle layers remained normal.

Lethal dosages of T-2 toxin (1.0 and 1.5 mg/kg) effected a marked disruption and injury to all cellular components of the intestine including the tunica muscularis. Massive, generalized edema was evidenced in all layers, notably in the lamina propria and submucosa which contained high concentrations of pycnotic leucocytes and focal areas of necrosis. Lysis and karyorrhexis of epithelial cells with cellular debris in the lumena of intestinal crypts was evidenced; villi were hyperemic and Peyers patches exhibited both central necrosis and also pycnosis in outer cortical lymphocytes. Nuclei of smooth muscle cells in the tunica muscularis were swollen, and the sarcoplasm exhibited focal areas of hyalinization and heterogeneity of staining. There was also severe serosal hemorrhaging, vascular congestion, and extensive disruption of both vascular and lymphatic endothelial cells. The severity of edema, extent of lymphoidal necrosis and related cytopathic changes in vascular, epithelial and stromal elements were generally more marked in the 1.5 mg/kg treatment group.

Time dependent alterations

Similar data obtained from rats injected ip with a 1.5 mg/kg dose and killed at 2 hr intervals over a 2 to 12 hour post-injection interval revealed that irreversible cytotoxic effects are evidenced in mucosal, submucosal, muscular and adventitial compartments as early as 2 h after T-2 treatment. For example at 2 h post-injection, all of the rats exhibited serosal hemorrhaging, disruption of vascular and lymphatic endothelium, necrosis of Peyers patches and both nuclear and cytoplasmic manifestations of cellular injury in stromal, epithelial and smooth muscle cell (SMC) components. Rats killed at subsequent time intervals over the 12 h time period simply revealed a more massive generalized edema, progressive destruction of all tissue components notably the lysis and denudation of epithelial cells in both crypts and villi, and increased numbers of cells exhibiting nuclear degeneration (karyorrhexis and karyolysis).

Summary of major findings

The overall data from the foregoing subprojects support the existence of marked differences in the susceptibility of various intestinal tissue components to T-2 toxin-induced injury. Of the cell types examined, a ranking of cells exhibiting cytopathic changes, arranged in decreasing order of susceptibility to T-2 toxin, is as follows: arterial endothelium, germinal center lymphocytes, intestinal crypt epithelium and villus epithelium, with lymphatic endothelium and SMC being the most resistant to T-2 toxin injury.

3. Adrenocortical Responses

Microscopic analyses of adrenocortical and medullary cells of acute T-2 toxin-treated rats revealed no nuclear or cytoplasmic evidence of cytotoxicity in any of the cortical zones or in chromaffin cells of the medulla.

Cytophotometric analysis of Feulgen-DNA levels also indicated the absence of any T-2 toxin-induced nuclear alterations since F-DNA levels of adrenocortical and medullary cell nuclei remained relatively constant irrespective of the dosage administered (Tables 17-20). No marked depletion of RNA or protein was evidenced in adrenals of T-2 toxin-treated groups; instead, in several instances, notably in zona glomerulosa (ZG)† cells and medullary cells, increases in RNA and were evidenced in the higher dosage groups. For example, in ZG cells which synthesize and secrete the mineralocorticoid, aldosterone, all T-2 toxin-treated groups exhibited an increase in RNA levels whereas protein levels generally remained within 10% of control values (Table 20). Adrenal medullary cells also exhibited moderate elevation in RNA levels of 16% and 19% in 1.0 and 1.5 mg/kg treatment groups, with slight increase (10%) in protein levels evidenced following a 1.0 mg/kg dose. On the other hand, in zona fasciculata† cells which synthesize glucocorticoids such as corticosterone, as well as in the reticular zone, both RNA and protein levels remained constant.

Table 17: Cytochemical Responses of the Adrenal Zona Glomerulosa in T-2 Toxin-Treated Rats

Treatment[a]	n[b]	RNA[c]	Δ%	Protein[c]	Δ%	F-DNA[c]
Control	120	57±33[2]		79±11[3]		15±2[1]
0.50 mg/kg	120	70±48[1]	+23	70±11[4]	-12	14±2[1]
0.75 mg/kg	120	71±48[1]	+25	83±11[2]	+ 5	15±2[1]
1.00 mg/kg	120	71±38[1]	+25	80±11[3]	+ 1	15±2[1]
1.50 mg/kg	120	63±32[2]	+10	87±14[1]	+10	15±4[1]

[a]T2 was administered ip in absolute ethanol. All rats were killed 8 hr post-injection.

[b]n, equals the number of individual cell measurements per stain per treatment group with the exception of the Feulgen-DNA(F-DNA) stained cells which were spot checked.

[c]Mean ± standard deviation in absorbancy units. Values with different superscripts are significantly different, $p < 0.05$ using Duncan's new multiple range test. Different stains are not comparable to one another.

Table I8: Cytochemical Responses of the Adrenal Zona Fasciculata in T-2 Toxin-Treated Rats

Treatment[a]	n[b]	RNA[c]	Protein[c]	Δ%	F-DNA[c]
Control	120	49±21[1]	72±11[1]		12±2[1]
0.50 mg/kg	120	50±26[1]	74±11[2,3]	+ 3	13±2[1]
0.75 mg/kg	120	51±25[1]	76±8[1,2]	5	12±1[1]
1.00 mg/kg	120	48±21[2]	79±11[1]	10	13±2[1]
1.50 mg/kg	120	47±19[1]	74±[2,3]		14±1[1]

[a]T2 was administered ip in absolute ethanol. All rats were killed 8 hr post-injection.

[b]n, equals the number of individual cell measurements per stain per treatment group with the exception of the Feulgen-DNA (F-DNA) stained cells which were spot checked.

[c]Mean ± standard deviation in absorbancy units. Values with different superscripts are significantly different, $p < 0.05$ using Duncan's new multiple range test. Different stains are not comparable to one another.

Table 19: Cytochemical Responses of the Adrenal Zona Reticularis in T-2 Toxin-Treated Rats

Treatment[a]	n[b]	RNA[c]	Protein[c]	F-DNA[c]
Control	120	66 ± 30[1]	67 ± 9[2]	15 ± 3[1,2]
0.50 mg/kg	120	68 ± 34[1]	60 ± 9[3]	14 ± 1[2]
0.75 mg/kg	120	64 ± 33[1]	60 ± 11[3]	16 ± 2[1]
1.00 mg/kg	120	71 ± 36[1]	75 ± 11[1]	14 ± 1[2]
1.50 mg/kg	120	71 ± 32[1]	69 ± 14[2]	16 ± 2[1]

[a]T2 was administered ip in absolute ethanol. All rats were killed 8 hr post-injection.

[b]n, equals the number of individual cell measurements per stain per treatment group with the exception of the Feulgen-DNA (F-DNA) stained cells which were spot checked.

[c]Mean ± standard deviation in absorbancy units. Values with different superscripts are significantly different, $p < 0.05$ using Duncan's new multiple range test. Different stains are not comparable to one another.

Table 20: Cytochemical Responses of the Adrenal Medulla in T-2 Toxin-Treated Rats

Treatment[a]	n[b]	RNA[c]	Protein[c]	F-DNA[c]
Control	120	32 ± 15^{1}	60 ± 8^{2}	12.0 ± 2^{2}
0.50 mg/kg	120	31 ± 14^{2}	57 ± 5^{1}	12.0 ± 2^{2}
0.75 mg/kg	120	$34 \pm 17^{1,2}$	55 ± 8^{3}	12.0 ± 2^{2}
1.00 mg/kg	120	37 ± 17^{1}	69 ± 10^{1}	12.0 ± 1^{2}
1.50 mg/kg	120	28 ± 16^{1}	63 ± 10^{2}	14.0 ± 2^{1}

[a]T2 was administered ip in absolute ethanol. All rats were killed 8 hr post-injection.

[b]n, equals the number of individual cell measurements per stain per treatment group.

[c]Mean ± standard deviation in absorbancy units. Values with different superscripts are significantly different, $p < 0.05$ using Duncan's new multiple range test. Different stains are not comparable to one another.

An additional aspect of work entailed examining the extent to which T-2 toxin elicits a stress mediated activation of the pituitary-adrenocortical axis leading to increased circulating levels of corticosterone. Based on data presented in Table 21 it is evident that subiethal doses of T-2 toxin effect a decrease in corticosterone levels (ca. 40%), whereas with lethal dosages of 1.0 to 1.5 mg/kg hormone levels are unchanged relative to control values at 8 h post-injection. In the time dependent study, it was also found that corticosterone levels are not elevated within the 2 to 8 h time-frame used in rats injected with 1.5 mg/kg i.p.

4. Nephrotoxic Effects of T-2 Toxin

Renal tubular nucleic-acid protein responses were also monitored in rats at 8 h following single injections of T-2 toxin (0.75, 1.0, 1.5 or 6.0 mg/kg ip); an additional group received a dose of 0.9 mg/kg and killed 7 d later. As in previous subprojects, alterations in cytochemical aspects of macromolecular metabolism were correlated with cytomorphological changes in renal components and cytopathic responses in other organ systems to determine whether T-2 toxin poisoning is associated with direct cytotoxic effects on proximal renal tubular epithelial cells.

Microscopic examination of H & E stained kidney sections revealed no evidence of necrosis nor any indication of incipient nuclear injury (e.g., pycnosis) in any of the T-2 toxin-treated rats; however, moderate tubular dilation and cytoplasmic vacuolization were evidenced with the higher T-2 toxin dosages (1.5 and 6.0 mg/kg).

Cytochemical studies confirmed the absence of any marked alterations in the physicochemical state of chromatin as reflected in the observation that the F-DNA yield of proximal tubular nuclei of T-2 toxin-treated groups remained at control levels (Table 22). On the other hand, a dose-dependent reduction in cellular RNA levels was evidenced, ranging from 7% with a 0.75 mg/kg to 43% with a 6.0 mg/kg challenge (Table 23); RNA contents were still moderately depressed (23%) at 7 d following a 0.9 mg/kg dose. Total cellular protein levels generally remained at control levels or in some instances exhibited a slight (10-13%) suppression in T-2 toxin-treated rats (Table 24).

In brief, the overall data fail to support the existence of direct nephrotoxic actions of T-2 toxin.

5. Lymphoidal Responses to T-2 Toxin

In addition to analyses of lymphoidal responses in the lamina propria of the intestine which were described in subsection 1, histologic and cytophotometric analyses of nucleic acid-protein responses were also conducted on thymus and spleen sections.

Table 21: Plasma Corticosterone Levels in T-2 Toxin-Exposed Rats

T-2 Toxin Treatment[a]	N[b]	Corticosterone Concentration[c]
Control	6	24 ± 2.4[2,3]
0.50 mg/kg	6	14 ± 1.5[4]
0.75 mg/kg	6	15 ± 1.5[4]
1.00 mg/kg	6	24 ± 1.9[2,3]
1.50 mg/kg	6	25 ± 2.7[2,3]
1.5 mg/kg at:		
2 hr	6	29 ± 1.6[1,2]
4 hr	6	30 ± 3.3[1,2]
6 hr	6	35 ± 3.8[1]
8 hr	6	25 ± 2.7[2,3]
Death	2	17 ± 1.5[3,4]

[a]T2 was administered ip in absolute ethanol. In the dose-dependent study, rats were killed 8 hr post-injection; in the time-dependent study, rats were killed at 2 h intervals as indicated.

[b]n, equals the number of animals within sample.

[c]Plasma corticosterone mean ± standard error in μg%. Values with different superscripts are significantly different, $p < 0.05$ using Duncan's new multiple range test.

Table 22. Proximal Tubule Cell Feulgen-DNA (F-DNA) Reactivity in T-2 Toxin-Treated Rats.

T-2 Toxin Treatment[a]	N(n)[b]	F-DNA Reactivity[c]
Control	6(100)	106 ± 11[1]
0.75 mg/kg	6(100)	105 ± 11[1]
1.0 mg/kg	6(100)	102 ± 12[1]
1.5 mg/kg	6(100)	110 ± 12[1]
6.0 mg/kg	6(100)	110 ± 12[1]
0.9 mg/kg	6(100)	107 ± 11[1]

[a]All animals were decapitated without anesthesia at 8 h, with the exception of the 0.9 mg/kg group which was killed at 7 d post-injection.

[b]N, number of animals per treatment group; n, number of individual cell measurements.

[c]Reaction product formation in Absorbancy Units (A.U.) ± Standard Deviation. Means with different superscripts are significant, $p < 0.05$, Duncan's multiple range test.

Table 23: Proximal Tubule Cell Azure B-RNA Content in T-2 Toxin-Treated Rats.

T-2 Toxin Treatment[a]	N(n)[b]	RNA Content[c]
Control	6(100)	122 ± 25[1]
0.75 mg/kg	6(100)	114 ± 16[2]
1.0 mg/kg	6(100)	89 ± 22[3]
1.5 mg/kg	6(100)	78 ± 18[4]
6.0 mg/kg	6(100)	69 ± 14[5]
0.9 mg/kg	6(100)	94 ± 16[3]

[a]Animals were killed at 8 h, with the exception of the 0.9 mg/kg group which was decapitated at 7 d post-exposure.

[b]N, number of animals per group; n, number of individual cell measurements.

[c]Proximal tubule cell azure B-RNA content (Absorbancy Units ± Standard Deviation). Means with different superscripts are significant, $p < 0.05$, Duncan's multiple range test. Means ranked (1-5), the highest designated as (1).

Table 24: Proximal Tubule Cell Mercuric Bromophenol Blue-Protein Content in T-2 Toxin-Treated Rats.

T-2 Toxin Treatment[a]	N(n)[b]	Protein Content[c]
Control	6(100)	124 ± 23[1]
0.75 mg/kg	6(100)	123 ± 23[1]
1.0 mg/kg	6(100)	112 ± 15[2]
1.5 mg/kg	6(100)	108 ± 12[2]
6.0 mg/kg	6(100)	124 ± 12[1]
0.9 mg/kg at 7 d	6(100)	126 ± 13[1]

[a]Animals were sacrificed at 8 h, with the exception of the 0.9 mg/kg group which was killed at 7 d post-injection.

[b]N, number of animals per group; n, number of individual cell measurements.

[c]Proximal tubule cell protein content in Absorbancy Units (A.U.) ± Standard Deviation. Means with different superscripts are significant, $p < 0.05$, Duncan's multiple range test. Means ranked (1-2), the highest designated as (1).

Although these analyses are still in progress, preliminary results indicate a dose-dependent increase in the severity of suppression of lymphopoiesis in splenic tissue but not in thymic tissue with considerable necrosis evidenced in B-dependent regions of the spleen (e.g., sinusoids of the red pulp and marginal zone of the white pulp).

6. Discussion and Conclusions

Extensive evidence supports that a major cellular mechanism of T-2 intoxication is an inhibition of protein synthesis. It has been postulated that most, if not all, of the observed cytopathic actions of T-2 toxin in multiple tissue compartments, are directly related to T-2 toxin-induced inhibition of protein and nucleic acid synthesis (1,2,17). On the other hand, specific cytochemical events which precipitate the onset of lesion formation, hemorrhaging and necrosis, have not yet been identified. Thus, the focus of the present study involved the use of microscopic cytochemical probes to identify specific sites of injury in the heart, brain and other systemic organs in rats following acute exposure to sublethal and lethal doses of T-2 toxin. A battery of cytochemical and morphometric indices of cytopathic responses, supplemented by biochemical analyses where deemed desirable was used to obtain a more comprehensive assessment of cardiovascular, neural and hormonal systemic interactions associated with T-2 toxin poisoning.

Among some of the specific contributions of the overall study include the following:

(1) Definitive evidence was obtained documenting that the heart constitutes a primary target site of T-2 toxin action; also that endothelial cell injury in the endocardial compartment constitutes the initial event which precipitates subsequent manifestations of cardiotoxicity.

(2) Supportive evidence was also obtained which indicates that vascular endothelial injury is an important cytotoxic event in tissues with a component of rapidly dividing cells (e.g., gut, lymphoid and hemopoietic tissues) which exhibit th most severe alterations following acute T-2 toxin treatment.

(3) Although acute T-2 toxin exposure is associated with an inhibition of RNA-protein synthesis in brain neurons, hepatocytes and renal tubular epithelial cells, the absence of irreversible cell injury and necrosis indicates these tissue compartments do not constitute primary or major target sites of T-2 mycotoxin action.

(4) Systemic events which participate in exacerbating cardiotoxic, vascular and enterotoxic pathogenic responses include a dose-dependent elevation in plasma histamine levels, release of vasoactive autacoids from mast cells and possibly an impairment in

homeostatic functioning of the hypothalamo-pituitary-adrenocortical axis.

(5) Most of the data relating to the pattern of chromatin, RNA and protein responses generally support the tenet that at the cellular level, the primary mode of action of T-2 toxin is an inhibition of protein synthesis, with RNA and chromatin changes occurring secondarily. On the other hand, the data also support the existence of marked differences among specific cell types within primary and secondary target tissue compartments in their susceptibility to cytotoxic actions of T-2 toxin.

Brief discussions of specific findings which support the above conclusions are presented below with respect to the functional significance of observed T-2 toxin-induced nucleic acid responses in various target tissue compartments.

With respect to cardiotoxic effects of T-2 toxin, the overall data support the following sequence of events which eventuate in cardiopathy. The initial site of injury is a disruption and damage to endothelial cells which in vitro studies indicate are several fold more susceptible to injury than smooth muscle cells. It is likely that the resultant increase in permeability results in a marked influx of T-2 toxin and other plasma constituents into the subendothelial compartment. It is noteworthy that even with sublethal dosages (0.75 mg/kg) there is a very marked protein depletion of myocardial cells. This is consistent with the cellular mode of action of T-2 toxin as a potent inhibitor of protein synthesis. The observation that RNA depletion and suppression of chromatin template activity (using F-DNA yield as an indicator of chromatin compaction) are not as severe as the extent of protein depletion also agrees with the current view that RNA and nuclear events occur secondarily to protein inhibition. In any event, the overall pattern of responses, i.e., a dose-dependent increase in the severity of myocardial edema and in the extent of protein and RNA inhibition which persists for 7 days after a single injection of T-2 toxin, indicates the heart constitutes a primary target site of T-2 mycotoxin action.

With respect to neurotoxic effects of T-2 toxin, neuronal protein levels were suppressed in a dose-dependent fashion within the cerebral cortex while in the striatum there was no direct correspondence between protein loss and T-2 toxin dosage at 8 h post-injection. Furthermore no hemorrhages or areas of necrosis were evidenced, and neuronal RNA levels were generally maintained at or near control levels. On the basis of these findings it was concluded that T-2 toxin does not elicit direct cytotoxic actions in these two brain regions. It is likely that neuronal protein depletion is attributable to systemic effects of T-2 toxin leading to cardiovascular insufficiency and hypoxemia. It is also probable that visceral pooling of blood would reduce the net amount of T-2 toxin reaching the brain thereby effectively decreasing the extent of injury to microvascular elements. In fact, it has been

suggested that overt CNS signs of trichothecene poisoning such as abnormal EEG's, coma and hallucinations probably stem from hypotension (18). Since oxygen lack reportedly comprises neuronal macromolecular biosynthetic activities (19), T-2 toxin-induced reductions in brain RNA/protein metabolism are probably secondary manifestations of cardiovascular insufficiency and hypoxemia. Other brain regions, however, need to be examined since several reports indicate that certain brain compartments such as the hypothalamus and associated catecholiminergic CNS compartments may be more sensitive to direct cytotoxic actions of T-2 toxin (20). It is noteworthy in this regard that T-2 toxin failed to elicit an increase in adrenocortical activity, whereas most xenobiotics and non-specific stress stimuli typically trigger a marked increase in corticosterone secretion. The absence of this hormonal response could stem from an impairment in hypothalamic functioning since there was no evidence of cellular injury in adrenocortical cells.

Our findings relating to enterotoxic effects of T-2 toxin generally confirm reports that the gut represents a primary target site of toxin action. The observation that intestinal compartments such as the crypt epithelium and germinal centers of Peyer's patches are most severely affected also supports current concepts that mitotically active cell populations are more susceptible than non-dividing cells to T-2 toxin-induced injury. On the other hand, it is clear that, as in the heart, the initial cytopathic event is endothelial cell injury in both serosal and mucosal regions as evidenced by a disruption of endothelial cell membranes, pycnotic nuclei, presence of edema in the interstitium and petechial hemorrhages within 2 h after T-2 toxin treatment. With lethal dosages of T-2 toxin, all cell components within mucosal, submucosal muscular and adventitial layers of the intestine exhibit cytopathic alterations. However, based on the severity of lesions with sublethal dosages a ranking of differential responsiveness of specific cell types (arranged in decreasing levels of susceptibility) is as follows: arterial endothelial cells, B- type lymphocytes comprising germinal centers, crypt epithelial cells, villus epithelium, T-type lymphocytes, fibroblasts, smooth muscle cells, lymphatic and venous endothelial cells.

Both the liver and kidney of T-2 toxin-treated rats exhibited moderate extents of cellular injury. However, neither organ exhibited focal areas of necrosis or hemorrhages in parenchymal or stromal compartments. For example, hepatocytes of liver lobules exhibited some reduction in basophilia, but only a moderate reduction in RNA levels and no depression in hepatocyte protein content. Similarly, despite a moderate suppression in renal tubular RNA levels, protein levels remained at near-normal levels or exhibited a slight (10-13%) decrease following exposure to lethal dosages. In both organs, nuclei of parenchymal cells remained euchromatic, healthy in appearance with no indication of a suppression in chromatin template

activity (i.e., low F-DNA stainability or chromatin compaction). Thus, it would appear that the liver and kidney, which represent the main organs involved in detoxification and excretion of trichothecene mycotoxins, are not primary target sites of T-2 toxicant action. It is likely that cytopathic changes such as reduced basophilia occur as a consequence of systemic responses, e.g., hypotension, hypoxemia and hypovolemia.

No morphological or cytochemical manifestations of cytotoxicity were evidenced in adrenocortical cells of T-2 toxin treated rats. It is well documented that noxious stimuli and/or injections of xenobiotics typically cause an activation of the hypothalamic-adrenocortical axis and a release of corticosterone. Such corticotropin mediated activation of the adrenal cortex usually results in an hypertrophy of inner fasciculate cells reflecting an enhancement in corticosterone synthetic capacity and vacuolization or degranulation of outer fasciculate cells associated with corticosterone release. Neither of these cytologic responses were evidenced in T-2 toxin challenged rats. This is also consistent with the finding that circulating corticosterone levels were maintained at normal levels or else moderately depressed with sublethal T-2 toxin dosages. We believe the absence of adrenocortical activation may stem from a T-2 toxin impairment in hypothalamic functioning since there was no histological evidence of a disruption of microvascular elements of the adrenal or indications of cytopathic alterations in any of the cortical zones. It is noteworthy that zona glomerulosa (ZG) cells which synthesize and release aldosterone were hypertrophic and contained elevated RNA levels. This is interpreted as reflecting a compensatory hormonal activation of ZG cells in response to T-2 toxin-induced hypovolemia and hypotension. In any event, it is clear that the adrenal cortex does not constitute a primary target site of T-2 cytotoxicity, at least with respect to a directly mediated toxin injury to adrenocortical cell elements.

Quantitative data were also obtained which indicate that an important aspect of acute T-2 toxin poisoning is a degranulation of mesenteric mast cells and a consequent release of vasoactive substances such as heparin, histamine and serotonin. Using diminution in metachromatic staining as an index of the severity of degranulation it would appear at first that sublethal dosages (0.5 and 0.75 mg/kg) are more efffective than lethal dosages in eliciting the release of autacoids. A more plausible explanation, however, is that with lethal dosages a high proportion of mast cells are completely degranulated and not identifiable as mast cells since they would be indistinguishable from fibroblasts using metachromatic stains. Recent studies by Yarom et al. (21) have implicated massive mast cell infiltration into subendocardial and subpericardial regions in the pathogenesis of ventricular myocardial fibrosis following chronic T-2 toxin poisoning. Thus, it would appear that in addition to direct cytotoxic injury to endothelial cells, vascular injury stemming from autacoid-mediated vasodilation exacerbates the extent of vascular congestion and proneness

to hemorrhaging in various target tissues. The reported presence of widespread focal hemorrhaging affecting many organs including the lungs, heart, subarachnoid vessels lends support to the belief that an anaphylactoid-type systemic response is a critically important aspect of the pathophysiological events which precipitate cardiopulmonary failure in mycotoxin poisoned animals.

Although analyses of splenic and thymic responses in acute T-2 toxin challenged rats are still in progress, preliminary examination of differentially stained sections have yielded a number of interesting results of particular relevance to the specific nature of T-2 toxin-induced immunosuppression. First, it was observed that the extent and severity of lesion formation is much more extensive in the spleen than in the thymus. Second, lymphocytoxic alterations in the spleen appear to primarily involve the red pulp and outer marginal zone of the white pulp region. Recent studies have shown that there is a topographical and functional zonation of lymphoidal tissue in the spleen with some areas containing predominantly B-type lymphocytes (red pulp) and other areas with T-lymphocytes (inner regions of white pulp surrounding the pulp artery). The designation of B or T cells refers to the maturation of certain lymphocytes in either the marrow or thymus where they acquire to the potential to form antibodies or cytotoxic lymphocytes, respectively. Thus, our data indicate that B-dependent spleen regions involved in mediating humoral (antibody) defense mechanisms are more severely affected by acute T-2 toxin poisoning than T-dependent regions. Interestingly, there was no marked involution or cell destruction evidenced in either cortical or medullary thymic compartments in T-2 toxin treated rats. Perhaps the existence of a blood-thymic barrier (which consists of a sheath of reticuloendothelial cells surrounding cortical capillaries) exerts a protective action in cortical regions. In any event, it is clear that during the acute phase of T-2 toxin poisoning, lymphoidal compartments primarily involved in mediating humoral (antigen-antibody) defense mechanisms are more severely compromised than the lymphocytic elements involved in cell-mediated cytotoxic or phagocytic immune responses.

In summary, an overview of observed tissue response patterns during acute T-2 toxin poisoning supports the following sequence of events which eventuates in lesion formation.

(1) Initially, T-2 toxin causes a disruption of the arterial-vascular endothelium resulting in a marked influx of plasma including toxin into the subendothelial interstitium.

(2) Concurrently, there is a marked widespread release of vasoactive substances into interstitial compartments which intensifies the extent of microvascular and vascular permeability changes. This is probably mediated via a direct T-2 toxin disruption of the plasma membrane of not only mast cells, but also of specialized intestinal epithelial cells (e.g., Paneth cells) resulting in a release of heparin, histamine, serotonin and related autacoids.

(3) The major sites of degenerative cellular changes and necrosis which occur subsequent to vascular congestion and edema are the germinal centers of Peyers patches presumed to contain proliferating B-lymphocytes and crypt al epithelial cells of the intestine. This agrees with expectations since tissues with a high component of dividing cells reportedly are most prone to T-2 toxin-induced injury.

(4) Especially with near-lethal or lethal dosages focal, widespread hemorrhages are evidenced in many organs including the lungs, intestines and heart. Several factors probably contribute to the lowered susceptibility of some organs and tissues to T-2 toxin-induced cytotoxicity. For example, low hemodynamic forces and lower susceptibility to toxin-induced injury of venous and lymphatic channels could explain the absence of marked hepatotoxic effects since liver parenchymal cells are bathed in an extensive matrix of simusoids. Also in some organs such as the thymus, a blood-thymic barrier probably limits the extent of T-2 toxin diffusion from capillaries to adjacent lymphocytic compartments.

(5) With respect to the cellular mode of action of T-2 toxin, in most of the target sites inhibition of protein synthesis appears to be the primary mechanism of cellular injury, since protein depletion is more severe and precedes suppression of RNA synthesis and/or inhibition of chromatin template activity. However, the cytotoxic effects of T-2 toxin on mast cells and arterial endothelial cells probably stem from a direct injury to the plasma membrane.

(6) During the acute phase of T-2 toxin poisoning, immunotoxic effects appear to largely involve the suppression of humorally mediated defense mechanisms since the onset of lesion formation is first evidenced in B-dependent lymphatic compartment.

LITERATURE CITED

1. Ueno, Y. (ed.) 1983. Trichothecenes: Chemical, Biological and Toxicological Aspects (Developments in Food Science 4). Elsevier, N.Y. 313 p.

2. McLaughlin, C.S., M.H. Vaughan, I.M. Campbell, C.M. Wei, M.E. Stafford and B.S. Hansen. 1977. Inhibition of protein synthesis by trichothecenes. p. 263-273. In: J.V. Rodricks, C.M. Hesseltine and M.A. Mehlman (eds.) Mycotoxins in Human and Animal Health. Pathotox Publishers, Park Forest South, Ill.

3. Talmage, D.W. (Chairman Committee on Protection Against Mycotoxins). 1983. Protection Against Trichothecene Mycotoxins. National Academy Press, Washington, D.C. 227 p.

4. Wied, G.L. and G.F. Bahr (eds.) 1970. Introduction to Quantitative Cytochemistry II. Academic Press, N.Y. 551 p.

5. Pattison, J.R., L. Bitensky and J. Chayen (eds.) 1979. Quantitative Cytochemistry and its Applications. Academic Press, N.Y. 322 p.

6. Anthony, A., T.M. Hollis, J.A. Penman, C. Zerweck and J.W. Doebler. 1981. Feulgen-deoxyribonucleic acid analysis of rabbit aortic smooth muscle cells using scanning-integrating microdensitometry. J. Histochem. Cytochem 29:1161170.

7. Martin, J.L., J.A. Doebler and A. Anthony. 1986. Scanning cytophocometric analysis of brain neuronal nuclear chromatin changes in acute T-2 toxin-treated rats. Toxicol. Appl. Pharmacol. 85:207-214.

8. Shea, J.R. 1970. A method of in situ cytophotometric estimation of absolute amount of RNA using azure B. J. Histochem. Cytochem. 18:143-152.

9. Martin, L.J., J.D. Morse and A. Anthony. 1986. Quantitative cytophotometric analysis of brain neuronal RNA and protein changes in acute T-2 mycotoxin poisoned rats. Toxicon (in press).

10. Bradford, M.M. 1976. A rapid and sensitive method for the quantitation of microgram quantities of protein utilizing the principle of protein-dye binding. Anal. Biochem. 72:248-254.

11. Mazia, D., P.A. Brewer and M. Alfert. 1953. The cytochemical staining and measurement of protein with mercuric bromophenol blue. Biol. Bull. 104:57-67.

12. Taylor, K.M. and S.H. Snyder. 1972. Isotopic microassay of histamine, histidine decarboxylase and histamine methyltransferase in brain tissue. J. Neurochem. 19:1343-1358.

13. Shaff, R.E. and M.A. Beaven. 1979. Increased sensitivity of the enzymatic isotopic assay of histamine: Measurement of histamine in plasma and serum. Anal. Biochem. 94:425-430.

14. Kelly, J.W. and G. Bloom. 1959. A quantitative spectrophotometric study of the mast cell. Exp. Cell Res. 16:538-564.

15. Doebler, J.A., T.-M. Shih and A. Anthony. 1985. Quantitative cytophotometric analyses of mesenteric mast cell degranulation in acute soman intoxicated rats. Experientia 41:1457-1458.

16. Shapiro, H. M. 1981. Flow cytometric estimation of DNA and RNA content in intact cells stained with Hoechst 33342 and pyronin Y. Cytometry 2:143-150.

17. Bamburg, J.R. 1983. Biological and biochemical actions of trichothecene mycotoxins. p. 41. In: F.E. Hahn (ed.), Progress in Molecular and Subcellular Biology. Berlin: Springer-Verlag.

18. Goodwin, W., C.D. Haas, C. Fabian, I. Heller-Bettinger and B. Hoogstraten 1978. Phase I evaluation of anguidine (diacetoxyscripenol, NSC 141537). Cancer 42:23.

19. Yanagihara, T. 1974. Cerebral anoxia: effect on transcription and translation. J. Neurochem. 22:13.

20. Cannon, M., W.I. Cranston, R.F. Hellon and Y. Townsend. 1982. Inhibition, by trichothecene antibiotics, of brain protein synthesis and fever in rabbits. J. Physiol., Lond. 322:447.

21. Yarom, R., R. More, S. Raz, Y. Shimoni, O. Sarel and B. Yagen. 1983. T-2 toxin effect on isolated perfused rat hearts. Bas. Res. Cardio. 78:623.

GLOSSARY

acidophilia - cytoplasmic affinity for acid dyes.

A.U. - absorbancy units. The total amount of absorbing material (chromophore) in a nucleus or cell is generally expressed in arbitrary photometric units and is a function of the extinction (optical density), the measured specimen area and the extinction coefficient of the dye used (see Bouger-Beer law of photometry).

autacoids - a functional term applied to class of diverse chemicals produced by cells which act as vasoactive mediators or inflammatory agents; examples include: histamine, serotonin, prostaglandins, leukotrienes and catecholamines.

azure B-RNA - complex of ribonucleic acid stained with the basic, thiazine dye, azure B (C.I. 52010, Allied Chem. Corp.). Since azure B binds to both DNA and RNA, total cellular RNA is measured cytophotometrically after the DNA is enzymatically removed by pretreatment of tissue sections with DNase prior to azure B staining.

azurophilia - nuclear and cytoplasmic affinity for azure B. Since nuclear azure B staining in non-dividing cell populations remains relatively constant and ribonucleoprotein is predominantly responsible for cytoplasmic azure B dye uptake, cytophotometric measures of the intensity of azurophilic staining can serve as presumptive indicators of RNA alterations within tissue compartments.

BAEC - bovine aortic endothelial cells

basophilia - nuclear and cytoplasmic affinity for basic dyes. The substance largely responsible for basophilic staining in the cytoplasm is ribonucleoprotein.

Bouger-Beer law of photometry - represents the basis for quantification in cytophotometry as in absorption colorimetry and is expressed as follows: $A = E = O.D. = \log (I_o/I_s) = -\log T = kMa = kcl$, where is the absorbancy (also referred to as extinction, E; or optical density, O.D.); I_o is the intensity of light after passing through the absorbing specimen; T is the transmission; k is the specific absorbancy of extinction coefficient of the chromophore (i.e., the azure B-RNA or F-DNA dye complex) at the defined wavelength; M is the mass of the chromophore in the measured field; a is the area of the measured cell or nucleus; c is the concentration of the chromophore; and l is the path length (i.e., section thickness) through the chromophore. In tissue sections, the relative amount of absorbing material (M) is determined from the product of the extinction and cellular or nuclear area, i.e., $M = Ea$ and is conventially expressed in integrated absorbancy units (A.U.).

In scanning methods, the incident light beam is a very small spot of light which is moved over the entire delimited region in a raster (flying-spot) pattern; within preset limits of the traverse, each light absorbing spot within an incremental area of the cell or nucleus is successively measured and integrated.

bromophenol blue-protein - refers to the use of mercuric bromophenol staining in the assay of protein content since this dye has an affinity for basic proteins and peptides that are not removed during tissue processing.

chromatin dispersion - refers to early changes in the physicochemical state of chromatin which presumably reflect the transformation of inactive chromatin segments into active templates for RNA synthesis. Among the changes in the deoxyribonucleoprotein (DNP) complex which reflect such activation include: increased susceptibility of chromatin to F-DNA acid hydrolysis, increased affinity of nuclear DNP for basic fluorescent dyes such as acridine orange and ethidium bromide and increase in nuclear volume. Since such changes precede RNA and protein synthesis, such DNP alterations reflect changes at the transcriptional level of cellular functioning.

chromophore - group of atoms in dye molecule responsible for the colored properties of the dye, i.e., the azo quinoid benzene ring in acid fuchsin or methyl violet. The terms "acid" or "basic" when applied to dyes do not refer to the hydrogen ion concentration but on whether a significant part of the dye is cationic (basic dye) or anionic (acid dye).

CNS - central nervous system.

compact or condensed chromatin - refers to those segments of chromosomes that are tightly coiled in the interphase nucleus; they are visible as more densely stained chromatin particles using basic dyes; such nuclei are frequently designated as "heterochromatic" by cytologists although the term heterochromatin has certain connotations to cytogeneticists which make the use of the prefixes hetero- and eu- less suitable for describing chromatin stainability or its appearance (see dispersed chromatin, chromatin activation).

Coomassie brilliant blue - stain used in spectrophotometric assay of cellular protein.

cytophotometry - (see microspectrophotometry and Bouger-Beer law of photometry).

DNA - deoxyribonucleic acid

DNase - deoxyribonuclease, a purified enzyme available commercially and used for preparing control slides in analyses of F-DNA content, Feulgen acid hydrolyzability of chromatin and in cytophotometric analysis of RNA.

DNP - deoxyribonucleoprotein complex consisting of DNA, histones and other proteins comprising chromatin.

F-DNA (Feulgen-DNA) content - designates the mean level of nuclear DNA measured cytophotometrically using the Feulgen reaction. Diploid DNA levels in nondividing cells are conventionally designated as containing 2C levels of DNA where C represents the haploid (germ cell) content. Proliferating cell populations in the synthsis (S) or postduplication (G2) interphase stages of the mitotic cycle contain intermediate (3C) and tetraploid (4C) contents of F- DNA. Slight departures from normalcy in the mean F-DNA level of 2C cells are attributable to alterations in the susceptibility of chromatin to acid hydrolysis and hence F-DNA staining.

Feulgen-DNA reactivity (F-DNA yield) - refers to the susceptibility of nuclear chromatin to acid hydrolysis; nuclei of metabolically inactive cells are generally more resistant to acid drolysis and exhibit a reduced intensity of Feulgen staining compared to 'active' cells; hence, shifts in the relative abundance of active to inactive cells leads to a skewness in the F-DNA frequency distribution profile of a population of nuclei (see chromatin dispersion, Feulgen reaction).

Feulgen reaction - reaction between colorless leucofuchsin (leuco-Schiff Reagent, C.I. 42500, Fisher) and aldehydes in deoxyribose which results in the formation of basic fuchsin (magenta or purple-blue color). Thus, tissue specimens are first hydrolyzed by HCl to free aldehyde groups of the pentose sugar of DNA and subsequently treated with leucofuchsin. DNA is Feulgen positive (magenta coloration); RNA is Feulgen negative.

interferometry - refers to the use of specially designed analytical interference microscopes such as the Mach-Zehnder Leitz interferometer to obtain precise measurements of section thickness within an accuracy of 0.02 μm or the mass of specified organic constituents within individual cells with a measuring accuracy of 10^{-14} g, i.e., 0.01 picograms

ip - refers to intraperitoneal injections.

LD_{50} - lethal dose fifty percent; refers to a specific dosage of a substance or toxin which kills fifty percent of the test organisms within a specified time period, i.e., 24 h, 48 h or 96 h.

metachromasia (syn. metachromasy) - refers to ability of certain basic (cationic) dyes such as azure B, toluidine blue and methylene blue, to stain certain tissue components with a different color from that of the original dye solution. Thus, mast cell granules are colored red-purple with azure B (metachromatic staining) whereas surrounding tissue elements are colored blue (orthochromatic).

microdensitomery (microspectrophotometry) - application of spectroscopic methods for the quantitative analysis of chemical constituents in tissue cells. Synonyms used include: cytophotometry, microphotometry and analytical microscopic cytochemistry or histochemistry.

pyronin Y - a fluorescent stain which can be used for quantification of RNA.

RNA - ribonucleic acid.

RNase - ribonuclease, a purified enzyme which is commercially available and used for preparing control slides in RNA analysis.

SMC - smooth muscle cells.

T-2 toxin - [3-d-hydroxy-4-β, 15-diacetoxy-8-α-(3-methylbutyryloxy)-12, 13 epoxytrichothec-9-en] - a highly toxic metabolite or mycotoxin produced by Fusarium poae, F. sporotrichioides and F. tricinctum.

zona fasciculata (ZF) cells - glandular epithelial cells of middle of adrenal cortex which synthesize and secrete glucocorticoids such as corticosterone; under the influence of anterior pituitary adrenocorticotropin.

zona glomerulosa (ZG) cells - outermost zone of adrenal cortex and site of synthesis and secretion of the mineralocorticoid, aldosterone; regulation of aldosterone secretion is primarily via the renin-angiotensin system and potassium concentration in response to hypovolemia and decrease in blood pressure.

DISTRIBUTION LIST

5 copies	Commander US Army Medical Research Institute of Infectious Diseases ATTN: SGRD-UIZ-M Fort Detrick, Frederick, MD 21701-5011
1 Copy	Commander US Army Medical Research and Development Command ATTN: SGRD-RMI-S Fort Detrick, Frederick, Maryland 21701-5012
12 copies	Defense Technical Information Center (DTIC) ATTN: DTIC-DDAC Cameron Station Alexandria, VA 22304-6145
1 copy	Dean School of Medicine Uniformed Services University of the Health Sciences 4301 Jones Bridge Road Bethesda, MD 20814-4799
1 copy	Commandant Academy of Health Sciences, US Army ATTN: AHS-CDM Fort Sam Houston, TX 78234-6100